6-15-2007

Analysis of Time-Series MODIS 250 m Vegetation Index Data for Crop Classification in the U.S. Central Great Plains

Brian D. Wardlow
University of Nebraska - Lincoln, bwardlow2@unl.edu

Stephen L. Egbert
University of Kansas, Lawrence, KS

Jude H. Kastens
Kansas Applied Remote Sensing Program, University of Kansas, Lawrence, KS

Published in *Remote Sensing of Environment* **108**:3 (June 15, 2007), pp. 290-310; doi 10.1016/j.rse.2006.11.021

Submitted March 15, 2006; revised November 7, 2006; accepted November 18, 2006;
published online January 18, 2007.

Analysis of time-series MODIS 250 m vegetation index data for crop classification in the U.S. Central Great Plains

Brian D. Wardlow,[a] Stephen L. Egbert,[b, c] and Jude H. Kastens [c]

[a] National Drought Mitigation Center, University of Nebraska–Lincoln, Lincoln, NE 68583, USA
[b] Department of Geography, University of Kansas, Lawrence, KS 66047, USA
[c] Kansas Applied Remote Sensing Program, University of Kansas, Lawrence, KS 66047, USA

Corresponding author — B. D. Wardlow, tel 402 472-6729, email bwardlow2@unl.edu

Abstract
The global environmental change research community requires improved and up-to-date land use/land cover (LULC) datasets at regional to global scales to support a variety of science and policy applications. Considerable strides have been made to improve large-area LULC datasets, but little emphasis has been placed on thematically detailed crop mapping, despite the considerable influence of management activities in the cropland sector on various environmental processes and the economy. Time-series MODIS 250 m Vegetation Index (VI) datasets hold considerable promise for large-area crop mapping in an agriculturally intensive region such as the U.S. Central Great Plains, given their global coverage, intermediate spatial resolution, high temporal resolution (16-day composite period), and cost-free status. However, the specific spectral–temporal information contained in these data has yet to be thoroughly explored and their applicability for large-area crop-related LULC classification is relatively unknown. The objective of this research was to investigate the general applicability of the time-series MODIS 250 m Enhanced Vegetation Index (EVI) and Normalized Difference Vegetation Index (NDVI) datasets for crop-related LULC classification in this region. A combination of graphical and statistical analyses were performed on a 12-month time-series of MODIS EVI and NDVI data from more than 2000 cropped field sites across the U.S. state of Kansas. Both MODIS VI datasets were found to have sufficient spatial, spectral, and temporal resolutions to detect unique multi-temporal signatures for each of the region's major crop types (alfalfa, corn, sorghum, soybeans, and winter wheat) and management practices (double crop, fallow, and irrigation). Each crop's multi-temporal VI signature was consistent with its general phenological characteristics and most crop classes were spectrally separable at some point during the growing season. Regional intra-class VI signature variations were found for some crops across Kansas that reflected the state's climate and planting time differences. The multi-temporal EVI and NDVI data tracked similar seasonal responses for all crops and were highly correlated across the growing season. However, differences between EVI and NDVI responses were most pronounced during the senescence phase of the growing season.

Keywords: MODIS, vegetation index data, crops, land used/land cover classification, U.S. Central Great Plains

1. Introduction

Land use/land cover (LULC) data are among the most important and universally used terrestrial datasets (IGBP, 1990) and represent key environmental information for many science and policy applications (Cihlar, 2000 and DeFries and Belward, 2000). The emergence of environmental change issues has generated critical new requirements for LULC information at regional to global scales. More accurate, detailed, and timely LULC datasets are needed at these scales to support the demands of a diverse and emerging user community (Cihlar, 2000; DeFries and Belward, 2000).

The environmental, economic, and social implications of LULC change have led to the recognition that LULC patterns must be mapped on a repetitive basis for large geographic areas in order to provide "up-to-date" LULC information and to characterize major human-environment interactions (National Aeronautics and Space Administration (NASA), 2002; National Research Council (NRC), 2001; Turner et al., 1995). As a result, the remote sensing community has been chal-

lenged to develop regional to global scale LULC products that characterize "current" LULC patterns, document major LULC changes, and include a stronger land use component. Several major research programs and documents, which include NASA's Land Cover–Land Use Change (LCLUC) program (NASA, 2002), the International Geosphere–Biosphere Program (IGBP)/International Human Dimensions Program (IHDP) Land Use/Land Cover Change (LUCC) Program (Turner et al., 1995), the National Research Council's (NRC) "Grand Challenges in Environmental Sciences" (NRC, 2001), and the U.S. Carbon Cycle Science Plan (Sarmiento & Wofsy, 1999) have identified the development of such LULC products as a research priority.

Improved and up-to-date LULC datasets are particularly needed for regions dominated by agricultural land cover such as the U.S. Central Great Plains. The cropland component of the agricultural landscape is of specific interest because it is intensively managed and continually modified, which can rapidly alter land cover patterns and influence biogeochemical and hydrologic cycles, climate, ecological processes, groundwater quality and quantity, and the economy. At the regional scale, cropland areas are characterized by a diverse mosaic of LULC types that change over various spatial and temporal scales in response to different management practices. As a result, detailed regional-scale cropping patterns need to be mapped on a repetitive basis to characterize "current" LULC patterns and monitor common agricultural LULC changes. Such information is necessary to better understand the role and response of regional cropping practices in relation to various environmental issues (e.g., climate change, groundwater depletion) that potentially threaten the long-term sustainability of major agricultural producing areas such as the U.S. Central Great Plains.

1.1. Remote sensing and large-area LULC mapping

Over the past decade, remotely sensed data from satellite-based sensors have proven useful for large-area LULC characterization due to their synoptic and repeat coverage. Considerable progress has been made classifying LULC patterns at the state (Eve & Merchant, 1998) and national (Craig, 2001; Homer et al., 2004; Vogelmann et al., 2001) levels using multispectral, medium resolution data from the Landsat Thematic Mapper (TM) and Enhanced Thematic Mapper (ETM+) as a primary input. Similar advances in LULC classification have also been made at national (Loveland et al., 1991; Lu et al., 2003) to global (DeFries et al., 1998; DeFries and Townshend, 1994; Hansen et al., 2000; Loveland and Belward, 1997; Loveland et al., 2000) scales using multi-temporal, coarse resolution data (1 and 8 km) from the Advanced Very High Resolution Radiometer (AVHRR). However, few of these mapping efforts have classified detailed, crop-related LULC patterns (Craig, 2001), particularly at the annual time step required to reflect common agricultural LULC changes. The development of a regional-scale crop mapping and monitoring protocol is challenging because it requires remotely sensed data that have wide geographic coverage, high temporal resolution, adequate spatial resolution relative to the grain of the landscape (i.e., typical field size), and minimal cost. Remotely sensed data from traditional sources such as Landsat and AVHRR have some of these characteristics, but are limited for such a protocol due to their spatial resolution, temporal resolution, availability, and/or cost.

Landsat TM/ETM+ data are appropriate for detailed crop mapping given the instruments' multiple spectral bands, which cover the visible through middle infrared wavelength regions, and 30 m spatial resolution. However, most crop classification using Landsat data has been limited to local scales (i.e., sub-scene level) (Mosiman, 2003; Price et al., 1997; Van Niel and McVicar, 2004; and Van Niel et al., 2005). Most state/regional-scale LULC maps derived from Landsat TM and ETM+ data, such as the United States Geological Survey's (USGS) National Land Cover Dataset (NLCD) (Homer et al., 2004; Vogelmann et al., 2001) and the Gap Analysis Program (GAP) datasets (Eve & Merchant, 1998), have classified cropland areas into a single or limited number of thematic classes and are infrequently updated. The exception is the United States Department of Agriculture (USDA) National Agricultural Statistics Service (NASS) 30 m cropland data layer (CDL), which is a detailed, state-level crop classification that is annually updated (Craig, 2001). However, the CDL is only produced for a variable and limited number of states (10 total states in 2004). The production of LULC datasets comparable to the CDL in other countries with large broad-scale farming systems is also lacking. The use of Landsat data (and data from similar sensors such as SPOT) for repetitive, large-area mapping has been limited primarily by the considerable costs and time associated with the acquisition and processing of the large number of scenes that are required. Data availability/quality issues (e.g., cloud cover) associated with acquiring imagery at optimal times during the year are also a factor (DeFries & Belward, 2000).

The value of coarse resolution, time-series AVHRR normalized difference vegetation index (NDVI) data for land cover classification at national (Loveland et al., 1991; Loveland et al., 1995) to global (DeFries et al., 1998; DeFries and Townshend, 1994; Hansen et al., 2000; Loveland and Belward, 1997; Loveland et al., 2000) scales has clearly been demonstrated. The high temporal resolution (e.g., 10 to 14-day composite periods, with near-daily image acquisition) of the time-series data coupled with the NDVI's correlation with biophysical parameters (e.g., leaf area index (LAI) and green biomass) (Asrar et al., 1989; Baret and Guyot, 1991) allows land cover types to be discriminated based on their unique phenological (seasonal) characteristics. The spectral–temporal information in time-series NDVI data also has been used to monitor vegetation conditions (Jakubauskas et al., 2002; Reed et al., 1996) and major phenological events (Reed et al., 1994; Zhang et al., 2003). However, the 1-km resolution limits the spatial and thematic detail of LULC information that can be extracted from AVHRR data. Most AVHRR pixels have an integrated spectral–temporal response from multiple land cover types contained within the 1 km footprint (Townshend and Justice, 1988; Zhan et al., 2002). As a result, coarse resolution sensors are appropriate for mapping "natural" systems, but the high spatial variability and complexity of agricultural systems requires higher resolution data than AVHRR provides (Turner et al., 1995). Most LULC classifications derived from 1 km AVHRR data emphasize broad scale natural vegetation classes and/or are comprised of "mixed" classes representing multiple LULC types. Cropland areas are typically represented as a generalized crop class or as a mixed crop/natural vegetation class.

1.2. The Moderate Resolution Imaging Spectroradiometer (MODIS)

The Moderate Resolution Imaging Spectroradiometer (MODIS) offers an opportunity for detailed, large-area LULC characterization by providing global coverage of science quality data with high temporal resolution (1–2 days) and intermediate spatial resolution (250 m) (Justice & Townshend, 2002). An "AVHRR-like" 250 m dataset is available at no cost, which includes a time series of visible red (620–670 nm) and near infrared (841–876 nm) surface reflectance, NDVI, and enhanced vegetation index (EVI) composited at 16-day intervals. The spatial, spectral, and temporal components of the MODIS 250 m VI data construct are appropriate for crop mapping and monitoring activities in the U.S. Central Great Plains. However, few studies have evaluated the potential of these data for detailed LULC characterization (Hansen et al., 2002; Wessels et al., 2004), particularly in an agricultural setting (Lobell and Asner, 2004; Wardlow et al., 2006).

The specific LULC information that can be extracted at the 250 m resolution is still relatively unexplored (Zhan et al., 2000). The 250 m bands were included in the MODIS instrument to detect anthropogenic-driven land cover changes that commonly occur at or near this spatial scale (Townshend & Justice, 1988). Land cover changes associated with anthropogenic and natural causes have been detected in the MODIS 250 m imagery (Hansen et al., 2002; Morton et al., 2006; Zhan et al., 2002). Wessels et al. (2004) found that general land cover patterns (e.g., agricultural, deciduous/evergreen forest, and grassland) could be successfully mapped with MODIS 250 m data. These results suggest that the MODIS 250 m data would be appropriate for crop mapping in the U.S. Central Great Plains given the region's relatively large field sizes. Fields are frequently 32.4 ha or larger, with such sites corresponding areally with approximately five or more 250-m MODIS pixels.

Two VIs, the NDVI and the EVI, are produced at 250-m resolution from MODIS. The NDVI is a normalized difference measure comparing the near infrared and visible red bands defined by the formula

$$\mathrm{NDVI} = (\rho_{\mathrm{NIR}} - \rho_{\mathrm{red}})/(\rho_{\mathrm{NIR}} + \rho_{\mathrm{red}}), \quad (1)$$

where ρ_{NIR} (846–885 nm) and ρ_{red} (600–680 nm) are the bidirectional surface reflectance for the respective MODIS bands. It serves as a "continuity index" to the existing AVHRR NDVI record. The EVI takes the form

$$\mathrm{EVI} = G((\rho_{\mathrm{NIR}} - \rho_{\mathrm{red}})/(\rho_{\mathrm{NIR}} + C_1 \times \rho_{\mathrm{red}} - C_2 \times \rho_{\mathrm{blue}} + L)), \quad (2)$$

where the ρ values are partially atmospherically corrected (Rayleigh and ozone absorption) surface reflectances, L is the canopy background adjustment ($L = 1$), C_1 and C_2 are coefficients of the aerosol resistance term that uses the 500 m blue band (458–479 nm) of MODIS (Huete et al., 1999) to correct for aerosol influences in the red band ($C_1 = 6$ and $C_2 = 7.5$), and G is a gain factor ($G = 2.5$) (Huete et al., 1994; Huete et al., 1997). The EVI is designed to minimize the effects of the atmosphere and canopy background that contaminate the NDVI (Huete et al., 1997) and to enhance the green vegetation signal (Huete et al., 2002). The MODIS VIs provide a consistent spatial and temporal coverage of vegetation conditions and complement each other for vegetation studies (Huete et al., 2002). Gao et al. (2000) found that the NDVI was more chlorophyll sensitive and saturated at high biomass levels, whereas the EVI was more responsive to canopy structure variations (e.g., LAI, plant physiognomy, and canopy type) and had improved sensitivity over high biomass areas.

Huete et al. (2002) evaluated the time-series MODIS 500 m and 1 km VI data products over several biome types (e.g., forest, grassland, and shrubland) and found that the multi-temporal signatures (or profiles) of both VIs well represented the phenology of each biome. However, the general EVI–NDVI relationship varied among the biomes and reflected differences in both their canopy structures and climate regimes. The two VIs were more strongly correlated for grassland and shrubland than for forests, and their dynamic ranges varied according to climate regime. Huete et al. (2002) also found that the EVI was more sensitive to variations over high biomass areas (e.g., tropical forest), whereas the NDVI tended to saturate. The response of the EVI and NDVI at the 250 m resolution and over cropped areas has yet to be evaluated and is a necessary first step in determining the suitability of these MODIS datasets for detailed crop characterization.

The objective of this study was to investigate the general applicability of the time-series MODIS 250 m EVI and NDVI datasets for crop-related LULC classification in the U.S. Central Great Plains. Initial results from other LULC characterization work using the MODIS 250 m VI data suggest that the spectral–temporal information in these data holds considerable potential for discriminating detailed crop classes based on their crop calendars (phenology). In this study, three primary research questions were addressed regarding the data's applicability for crop classification. First, do the time-series MODIS 250 m VI data have sufficient spatial, spectral, and temporal resolution to discriminate the region's major crop types (alfalfa, corn, sorghum, soybeans, and winter wheat) and crop-related land use practices (double crop, fallow, and irrigation)? Second, are the regional variations in climate and management practices (e.g., planting times) that occur across the study area detected in the time-series MODIS 250 m VI data for the crop classes? Third, how do the EVI and NDVI respond over the various crop cover types and how informationally distinct are the VIs in this setting? To address these questions, a combination of graphical and statistical analyses was performed on a 12-month time series of MODIS 250 m EVI and NDVI data (January to December) from 2179 cropped field sites across the state of Kansas.

2. Study area

Kansas (Figure 1), which is situated approximately between 37° and 40°N latitude and 94° and 102°W longitude, is an agriculturally dominated state that occupies 21.3 million ha of the U.S. Central Great Plains. A cropland/grassland mosaic comprises most of the state, with 46.9%

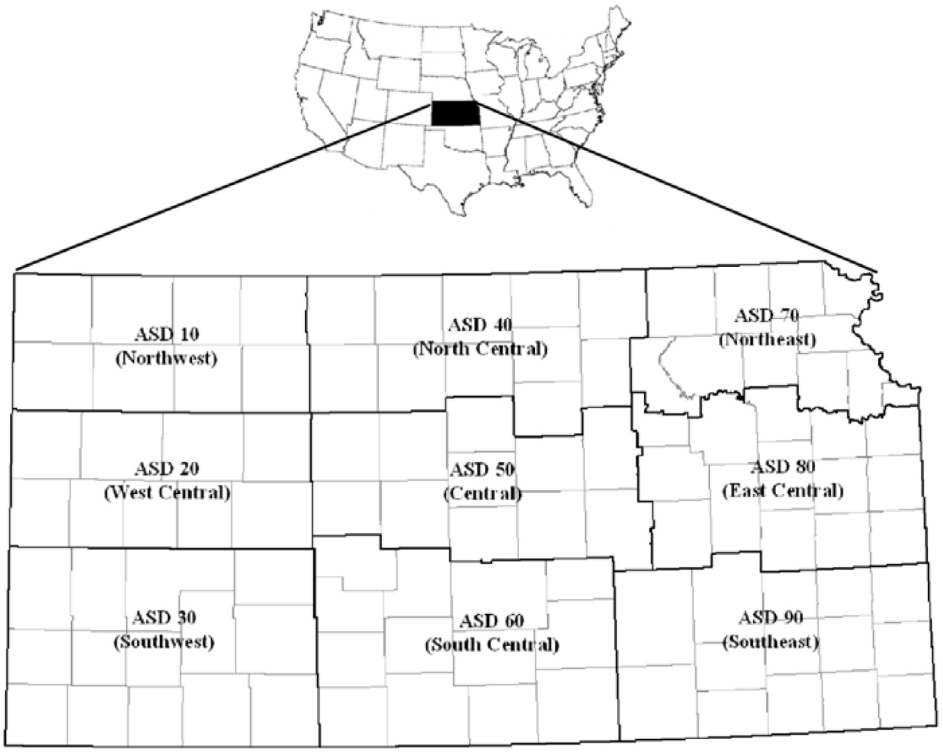

Figure 1. The state of Kansas study area map and USDA NASS Agricultural Statistics District (ASD) boundary map. The lighter line work corresponds with county boundaries.

(10.0 million ha) of its total area dedicated to intensive crop production. Cropland areas primarily consist of a mosaic of relatively large fields (~ 32.4 ha or larger) with diverse crop types and management practices that are representative of the larger U.S. Central Great Plains region. The state's major crop types are alfalfa (*Medicago sativa*), corn (*Zea mays*), sorghum (*Sorghum bicolor*), soybeans (*Glycine max*), and winter wheat (*Triticum aestivum*). Each crop has a well-defined crop calendar with specific planting times and unique seasonal growth patterns. The multi-temporal VI profile of each crop should reflect these unique phenological characteristics if the time-series MODIS VI data have sufficient resolution for crop class discrimination. However, each crop class may have several unique intra-class VI profiles that reflect the state's regional variations in environmental conditions and/or crop management practices.

Kansas has a pronounced east–west precipitation gradient that ranges from approximately 500 mm/year in the west to 1000 mm/year in the east (precipitation values reflect annual averages from 1961 to 1990). Semi-arid western Kansas commonly experiences severe drought events due to its limited and highly variable precipitation regime. Consequently, a considerable proportion of cropland in this area is irrigated from aquifers to maintain high crop production levels. It is expected that crops should exhibit distinctive irrigated and non-irrigated VI profiles, particularly in the semi-arid areas, due to the differential effects of drought stress on crops under these different management practices. Non-irrigated crops are also expected to have regional VI profile variations between eastern and western Kansas due to substantial precipitation differences. The climatic conditions of the 2001 growing season for Kansas were not extreme in terms of severe drought or excessive rainfall. The USDA (2002) reported that annual precipitation totals for most parts of Kansas were generally within 25–75 mm of their 10-year average, and therefore the 2001 growing season conditions were assumed to reflect the state's average climate patterns.

The average planting time for many crops in Kansas can differ by more than 1 month along a general southeast (earliest) to northwest (latest) gradient (Shroyer et al., 1996). For example, corn has a recommended planting date range from March 25 to April 25 for southeast Kansas and April 20 to May 20 for northwest Kansas (Shroyer et al., 1996). As a result, a crop like corn may have region-specific multi-temporal VI profiles that are temporally offset by as much as 1 month across the state.

3. Data description and processing

3.1. Time-series MODIS VI data

A 12-month time series of 16-day composite MODIS 250 m EVI and NDVI data (MOD13Q1 V004) spanning one growing season (January–December 2001) was created for Kansas. The time series consisted of 23 16-day composite periods, and three tiles (h09v05, h10v05, and h10v04) of the MODIS data were required for statewide coverage. For each composite period, the EVI and NDVI data were extracted by tile, mosaicked, and reprojected from the Sinusoidal to

the Lambert Azimuthal Equal Area projection. Time-series EVI and NDVI data were extracted and analyzed from field sites of specific crop types and management practices across Kansas.

3.2. Field site database

A database of field site locations, which were representative of Kansas' major crop types and cropping practices, was created using information from annotated aerial photos provided by the USDA Farm Service Agency (FSA). The FSA provided photos for 2179 individual fields throughout Kansas that were 32.4 ha or larger. The fields were distributed across 48 counties (of a total of 105 counties) in the state's major crop-producing areas to make sure that an adequate number of field sites was collected for each crop class and that the sites represented the intra-class variations related to climate and crop management practices. A minimum field size of 32.4 ha (equivalent in area to approximately five 250-m pixels) was selected to ensure that the fields were of sufficient size to be represented by multiple pixels in the 250 m imagery. The majority of fields were 40.5 ha or larger, with most of the smaller fields restricted to the rare classes and to sites in eastern Kansas, which typically have smaller field sizes.

Each field was located on the MODIS imagery using a georeferenced Public Land Survey System (PLSS) coverage and Landsat ETM+ imagery. A single 250-m pixel located completely within the field's boundaries was selected to represent each field site, and the corresponding time-series EVI and NDVI values for the pixel were extracted. A single, "maximally interior" pixel was used to minimize the potential of "mixed" pixels (comprised of multiple land cover/crop types) being included in the database. The MODIS data have high sub-pixel geolocational accuracy (± 50 m (1σ) at nadir (Wolfe et al., 2002)), so the influence of VI changes due to geometric inaccuracies between observations in the time series should be minimal. Table 1 presents the number of field sites by crop type and irrigated/non-irrigated status, and Figure 2 shows their geographic locations.

4. Methods

Several graphical and statistical analyses were performed to evaluate the applicability of the time-series MODIS 250 m VI datasets for crop discrimination. First, MODIS 250 m and Landsat ETM+ 30 m imagery were visually compared to examine the spatial cropping patterns that could be resolved at the 250 m resolution in the U.S. Central Great Plains.

Table 1. Number of irrigated and non-irrigated field sites by crop type

	Irrigated	Non-irrigated	Total
Alfalfa	124	119	243
Corn	330	279	609
Sorghum	35	319	354
Soybeans	235	219	454
Winter wheat	90	356	446
Fallow	0	73	73
Total	814	1365	2179

Second, the field sites were aggregated by crop type and management practice, and average, state-level multi-temporal VI profiles were calculated for each thematic class. The crop VI profiles were then visually assessed and compared to their respective crop calendars to determine if each crop's unique phenological behavior was detected in the time-series VI data. VI profiles were also visually compared for irrigated and non-irrigated crops, as well as fallow and double-cropped fields, to determine if unique multi-temporal VI signatures could be detected for these major land use classes.

Third, class separability between specific crop types in the time-series VI data was investigated using the Jeffries–Matusita (JM) distance statistic (Richards and Jia, 1999), which was demonstrated in Van Niel et al. (2005) to be an effective measure for this task. The JM distance between a pair of class-specific probability functions is given by

$$\mathrm{JM}(c_j,c_k) = \int_x \left(\sqrt{p(x|c_j)}-\sqrt{p(x|c_k)}\right)^2 \mathrm{d}x \tag{3}$$

In our study, x denotes a span of VI time series values, and c_j and c_k denote the two crop classes under consideration. Under normality assumptions, Equation (3) reduces to $\mathrm{JM} = 2(1 - e^{-B})$, where

$$B = \frac{1}{8}D^2 + \frac{1}{2}\ln\left(\left|\frac{\sum_j+\sum_k}{2}\right| \Big/ \sqrt{\left|\sum_j\right|\left|\sum_k\right|}\right)$$

$$\text{and } D^2 = (\mu_j-\mu_k)^T\left(\frac{\sum_j+\sum_k}{2}\right)^{-1}(\mu_j-\mu_k).$$

In this notation, μ_j and μ_k correspond to class-specific, expected VI values, and $\sum_j$ and $\sum_k$ are unbiased estimates for the class-specific covariance matrices. The JM distance, which can range between 0 and 2, provides a general measure of separability between two classes based on the average distance between their class density functions. A larger JM distance indicates more distinct distributions between two classes, which favors successful class discrimination. For this research, we examined both the full growing season and period-by-period JM distances for each pair of crop classes to determine their overall separability and understand how that separability changes over the growing season. The full growing season defined for this analysis spanned from the March 22 to the November 1 composite period. This time span was selected because it encompasses most of the crops' growth cycles. Conventional statistical methods (e.g., analysis of variance (ANOVA)) used to test for significant differences in the VI data between specific crops by composite period were not presented, because such tests often produced significant results due to the large number of class samples, which was not useful for this study (similar findings were presented in Van Niel et al., 2005). As a result, visual assessment in combination with the JM distance metric, which provides a flexible and intuitive separability index, were believed to provide better measures of the general separability of specific crop types throughout the year in the time-series VI data.

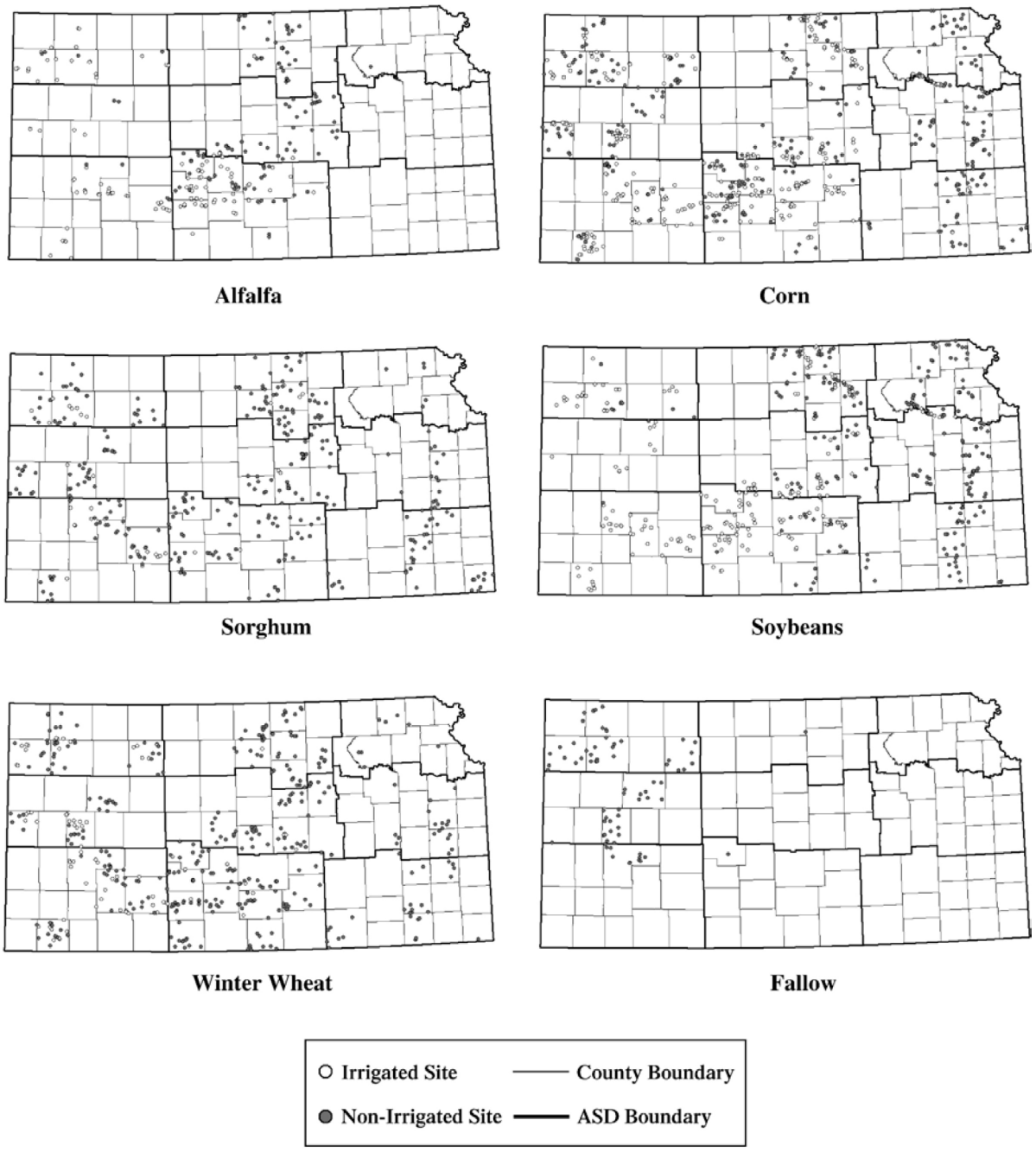

Figure 2. FSA field site locations by crop type and irrigated/non-irrigated status.

Fourth, the field sites were aggregated by USDA NASS Agricultural Statistics District (ASD) (Figure 1), and average ASD-level VI profiles were calculated and compared for each crop to assess their intra-class regional variations expressed in the MODIS data across Kansas. ASDs were an appropriate spatial unit for this type of comparison because they represent "agronomically defined" subdivisions of the state, which have relatively homogeneous cropping practices and environmental conditions (USDA, 2004). Comparisons were made only between Kansas' four "corner" ASDs—ASD 10 (northwest), ASD 30 (southwest), ASD 70 (northeast), and ASD 90 (southeast)—because they represent the extremes of the state's precipitation and planting time gradients, which would be the most likely drivers of regional variations in the crop-specific VI responses.

Finally, the general seasonal behaviors of the multi-temporal EVI and NDVI profiles over the growing season were assessed for each crop class through a series of analyses. Multi-temporal EVI and NDVI profiles were visually evaluated for each crop to identify any differences in their respective responses. Period-by-period JM distances and VI value differences were then calculated between the VIs to

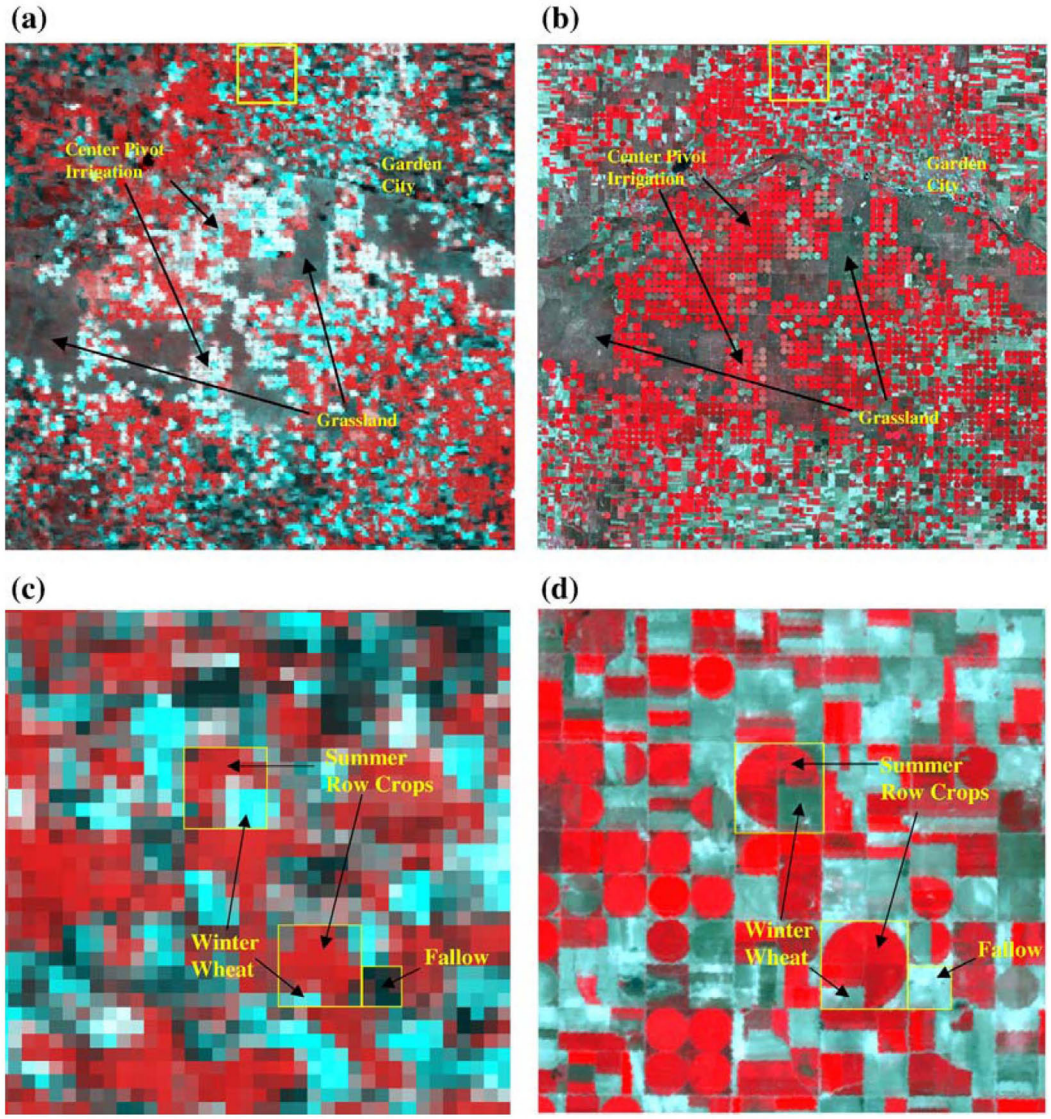

Figure 3. A visual comparison of multi-temporal MODIS 250 m NDVI imagery (NDVI from April 7, 2001 assigned to blue and green color guns and NDVI from July 28, 2001 to the red color gun) and single date, multi-spectral Landsat ETM+ 30 m imagery (false-color composite acquired on July 28, 2001) in an area of southwest Kansas. At the landscape level, the large grassland tracts and general cropping patterns are clearly seen in both the MODIS (a) and ETM+ (b) images. At the field level (c and d), many individual fields and blocks of fields planted to the same crop type can be identified in both the MODIS (c) and ETM+ (d) images. This is illustrated in the highlighted sections where the summer row crops, which comprise most of the fields under circular center pivot irrigation, can be distinguished from the fields planted in winter wheat.

determine their specific differences across the year. Correlation analysis was also conducted between the VIs during the greenup and senescence phases, and for irrigated and non-irrigated sites, to assess their relationship seasonally and by management practice. For seasonal analysis, the VIs were correlated for an equal number of periods for both phases and the specific temporal window of each phase was defined according to each crop's phenology. The greenup phase was defined as April 23 to July 12 for the summer crops, March 6 to July 12 for alfalfa, and March 6 to May 9 for winter wheat. Their senescence phases were defined as July 12 to September 30, July 12 to November 19, and May 9 to July 12, respectively. Although the correlations were based on a limited number of points (either 5 or 9 periods), they were considered representative of each crop's VI response because of the large, reliable sample of VI observations per composite period. Crossplots were also used to assess the general EVI–NDVI relationship across the year.

5. Results and discussion

5.1. MODIS 250 m imagery and agricultural LULC patterns

Figure 3 illustrates the potential of MODIS 250 m data for detecting crop-related LULC patterns in the U.S. Central Great Plains. Similar LULC patterns were detected in the multi-temporal MODIS 250 m and single date, multi-spectral Landsat ETM+ imagery at the landscape level (Figure 3a and b). General land cover types (e.g., grassland and cropland), specific crop types (e.g., winter wheat and summer crops), and cropland under center pivot irrigation were visually ev-

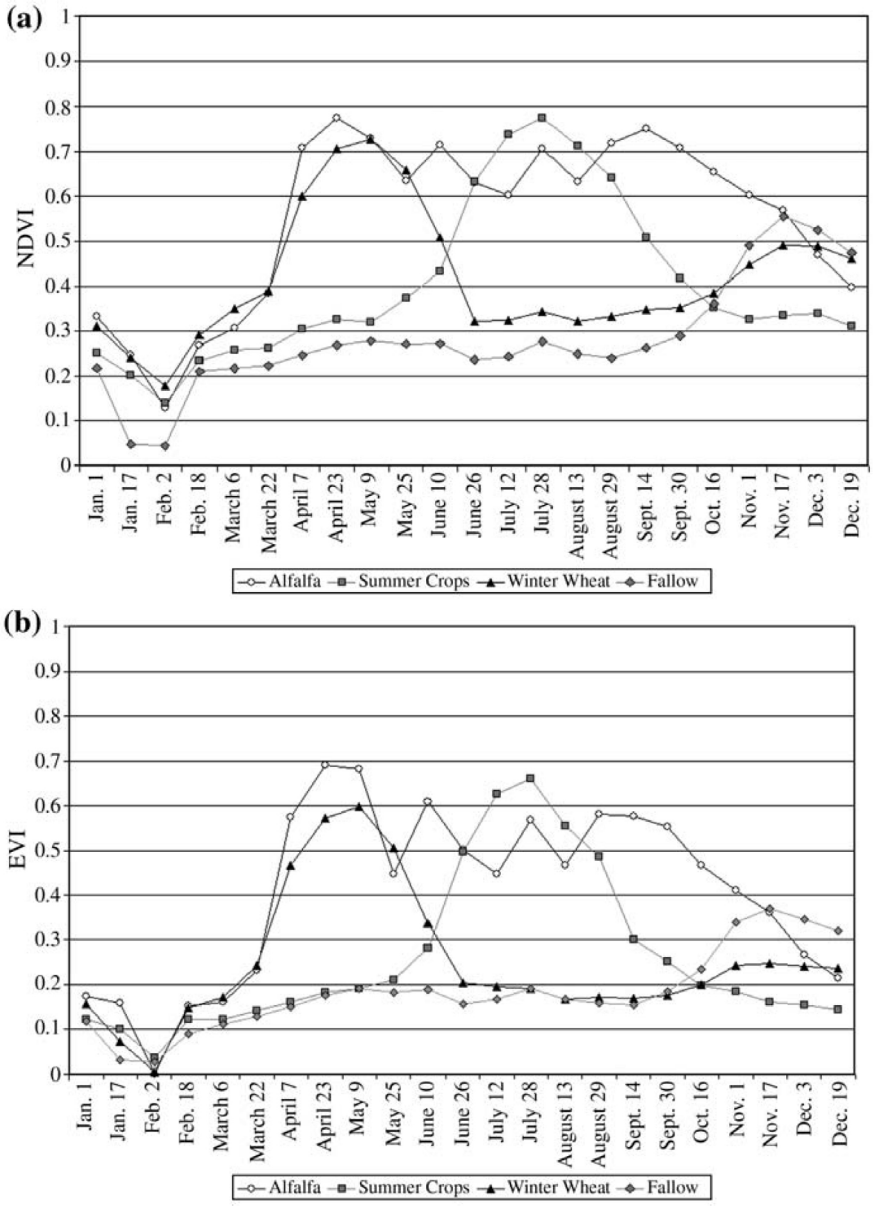

Figure 4. Multi-temporal NDVI (a) and EVI (b) profiles (state average) of the major crop categories in Kansas. Unique seasonal VI responses were detected in the MODIS 250 m data for alfalfa (number of fields n = 243), fallow (n = 73), summer crops (n = 1417), and winter wheat (n = 446).

ident in both images. Figure 3a also shows the value of the multi-temporal information in the MODIS NDVI image for crop discrimination as compared to the single-date of multi-spectral Landsat ETM+ imagery. Summer crops (red) and alfalfa (white) were separable in the MODIS image due to their different spring (April 7) and mid-summer (July 28) spectral responses, whereas both crops were spectrally similar (red) in the summer date (August 27) of Landsat ETM+ imagery. A closer, field-level comparison of MODIS and Landsat ETM+ images (Figure 3c and d) reveals that similar cropping/field patterns were represented in both images. Within the two highlighted sections (each 260 ha in size), fields planted to winter wheat, summer crops, and fallow could be visually identified in both the MODIS 250 m and Landsat 30 m imagery for fields at least 32.4 ha in size.

5.2. Multi-temporal VI profiles and crop phenology

The next phase was to determine if unique spectral–temporal responses were detected at the pixel-level in the time-series MODIS VI data for each crop class. The multi-temporal VI profile of a specific crop would be expected to reflect the crop's general phenological characteristics (e.g., timing of greenup, peak greenness, and senescence) if the data have sufficient spatial, spectral, and temporal resolution. In this section, the average multi-temporal VI profiles of crop types and crop-related land use classes (Figures 4–7) were visually assessed and compared to each class's documented crop calendar. Regional variations in each crop's multi-temporal VI signatures across Kansas were also considered.

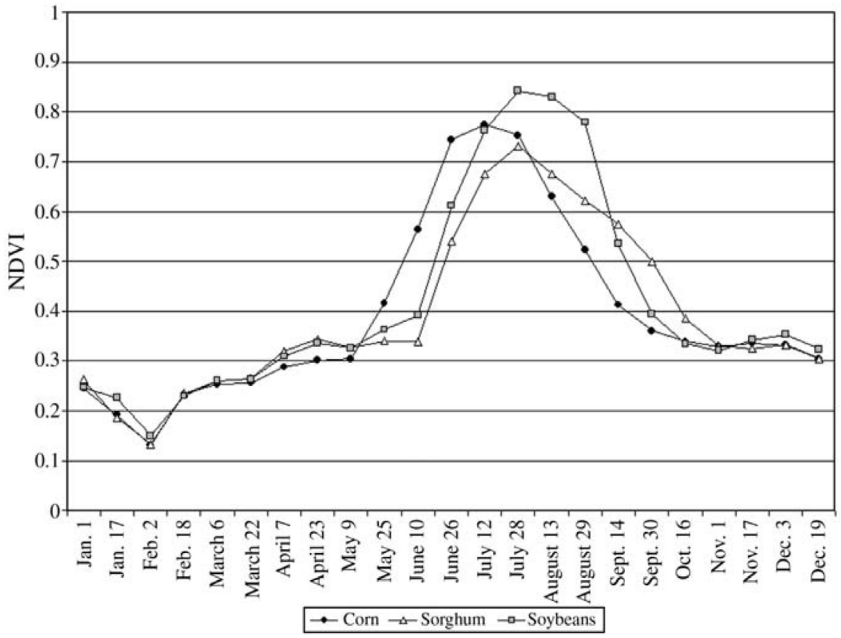

Figure 5. Multi-temporal NDVI profiles (state average) of corn (number of fields n = 609), sorghum (n = 354), and soybeans (n = 454) all exhibited a mid-summer peak NDVI, but the crops exhibited subtle differences in their respective VI responses across the growing season.

5.2.1. General crop types

Each general crop type had unique, well-defined multi-temporal NDVI (Figure 4a) and EVI (Figure 4b) profiles, and clear spectral–temporal differences appeared among the crops. Summer crops (i.e., corn, sorghum, and soybeans) had mid-summer (July and August) peak VI values (i.e., peak greenness), while the peak VI values of winter wheat occurred in the spring (late April–early May). Alfalfa maintained high VI values across a broad growing season, whereas the fallow fields maintained low VI values during that same period due to their unplanted state. A more in-depth discussion of the VI profile-crop calendar comparison is provided in this section for each crop class. This discussion is limited to only the NDVI profiles because both VIs exhibited a similar seasonal behavior for each crop as demonstrated in Figure 4a and b. An EVI–NDVI comparison is presented later in the paper for each crop type.

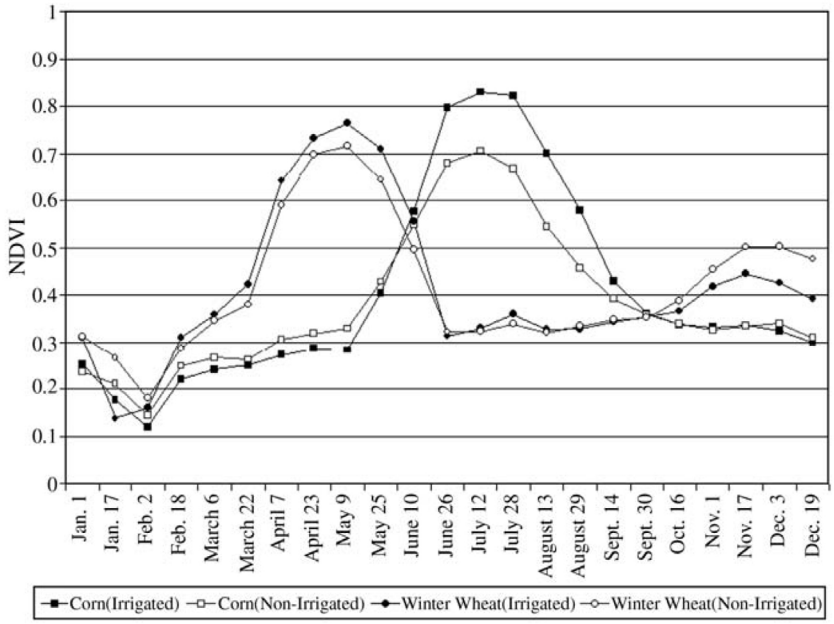

Figure 6. Irrigated crops had a higher peak NDVI and maintained a higher NDVI during each crop's growth cycle than non-irrigated crops as shown for corn (irrigated n = 330 and non-irrigated n = 279) and winter wheat (irrigated n = 90 and non-irrigated n = 356).

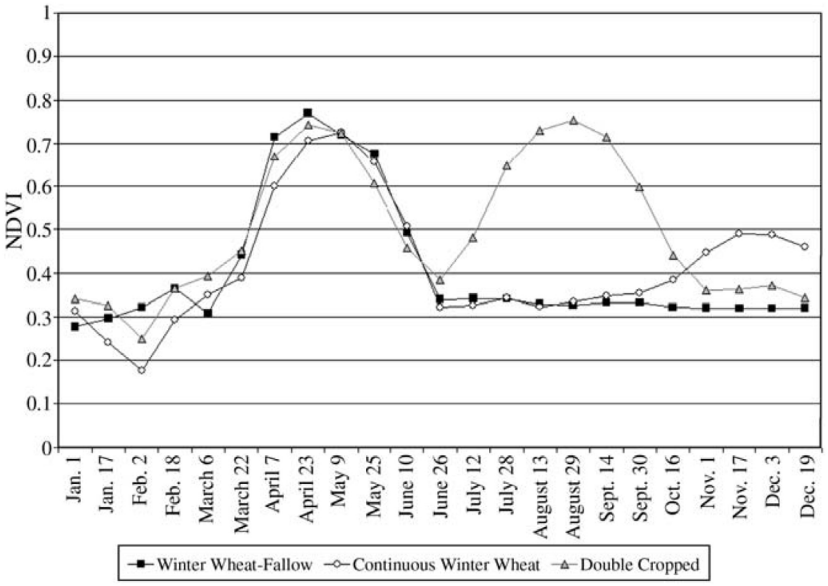

Figure 7. Distinct multi-temporal NDVI responses during the second half of the growing season were observed for three major winter wheat-related crop rotation sequences in the MODIS 250 m data.

5.2.2. Alfalfa

Alfalfa's phenology and characteristic "growth and cut" cycles were clearly detected in the time-series NDVI data (Figure 4a). Alfalfa is a perennial crop that breaks winter dormancy and begins photosynthetic activity/growth in March and early April (Shroyer et al., 1998), which was represented by the rapid NDVI increase (from 0.38 to > 0.70) between the March 22 and April 7 composite periods. Alfalfa is typically cut three or four times per year in Kansas, with the first cutting in late May or early June and a 4- to 5-week regrowth period between cuttings (Shroyer et al., 1998). The NDVI fluctuations throughout the growing season correspond well with three growth and cut cycles, though it is not known if the 2001 crop demonstrated typical statewide synchronization or if it was exceptional in this regard. The NDVI decrease (from 0.78 to 0.63) during the May 25 composite period was consistent with the general timing of the first cutting (Shroyer et al., 1998). This was followed by an NDVI increase (to 0.72) during the June 10 period, corresponding to a regrowth phase. Two additional cutting (July 12 and August 13) and regrowth (July 28 and August 29) cycles were reflected in the NDVI data during the remainder of the year. The gradual NDVI decrease from October through December corresponded to the general timing of senescence and the onset of winter dormancy for alfalfa.

5.2.3. Winter wheat

The winter wheat NDVI profile characteristics (Figure 4a) were consistent with the crop's distinctive crop calendar. Winter wheat is planted and emerges in the fall (October and November) before becoming dormant over the winter (Paulsen et al., 1997). Low NDVI values (~ 0.30–0.35) from January through mid-March reflect this winter dormancy. Winter wheat in Kansas resumes growth in the early spring (typically mid-March to early April) when the air and soil temperatures warm (Paulsen et al., 1997), which was represented by the rapid NDVI increase between the March 22 and April 7. Winter wheat's ripening and senescence phase occurs in late May and June (Paulsen et al., 1997), expressed by the rapid NDVI decrease (~ 0.70 to 0.30) during this time. Following the late June harvest, the winter wheat sites maintained a low NDVI value (~ 0.30) for the remainder of the summer, which reflects the non-vegetated spectral response of the soil and crop residue from the fields. A second, smaller NDVI peak (~ 0.50) appeared in November and December, corresponding to the emergence and growth of the next year's winter wheat crop. This secondary response was expected because for any given year, an appreciable fraction of the winter wheat fields in Kansas is continuously cropped in this fashion.

5.2.4. Summer crops

Corn, sorghum, and soybeans are categorized as "summer" crops because most of their growth cycle occurs during the summer. Although these summer crops have similar crop calendars, unique spectral–temporal responses that represent subtle differences in their growth cycles were reflected in their respective multi-temporal MODIS NDVI profiles (Figure 5).

Planting date differences among the summer crops were depicted by the different timings of their initial greenup (or NDVI increase) in the spring. Corn is the earliest planted summer crop (April to mid-May), followed by soybeans (mid-May to mid-June) and sorghum (late May to late June) (Shroyer et al., 1996). In the MODIS NDVI data, corn had the earliest greenup, between the May 9 and May 25 composite periods, followed by soybeans (approximately June 10) and sorghum (between June 10 and June 26).

The timing and value of the peak NDVI also varied among the summer crops. Corn peaked during the July 12 period with an intermediate NDVI value (0.77). Sorghum peaked during the July 28 period with a lower NDVI value (0.73). Soy-

beans peaked at the same time as sorghum and had the highest NDVI value (0.84). These peak growing season differences likely represent differences in the general growth/development pattern and canopy structure of the three crops.

The NDVI profiles of the three summer crops also exhibited different behaviors during the senescence phase of the growing season. The mid to late August onset of senescence for corn (Vanderlip & Fjell, 1994) was represented by the large NDVI decrease that began during the August 13 composite period and continued until mid to late September. Soybeans maintained a high NDVI (0.77) through August 29 and exhibited a rapid NDVI decrease beginning in early September and continuing until the beginning of October. This timing is consistent with the senescence of soybeans, which experience rapid desiccation, chlorophyll loss, and leaf drop during mid to late September (Rogers, 1997). Sorghum exhibited a gradual NDVI decrease over a 2-month period (approximately spanning the August 13 to October 16 composite periods), which reflects the extended period required by sorghum to dry and reach harvest maturity following its physiological maturity (Vanderlip et al., 1998).

5.2.5. Fallow

Fallowing is a dryland farming technique in which fields remain unplanted (idle) for most or all of a growing season in order to conserve soil moisture for crop production the following year (Havlin et al., 1995). Although fallow is not a crop, it must be represented in a crop classification scheme for the U.S. Central Great Plains because it is a widely used farming practice in the semi-arid parts of the region (e.g., western Kansas). Low NDVI (< 0.30) from January 1 to September 30 indicates the largely non-vegetated signal (crop stubble, soil, and sporadic weed cover) of these idle fields (Figure 4a). The NDVI increase (to 0.54) detected in mid-October to mid-November was associated with the emergence of winter wheat planted for the next year.

5.2.6. Irrigated vs. non-irrigated crops

As expected, irrigated crops had a higher peak NDVI and maintained higher NDVI values throughout most of each crop's growth cycle as demonstrated for corn and winter wheat in Figure 6. The NDVI difference was more pronounced during the summer than the spring. Irrigated winter wheat had NDVI values from 0.04 to 0.05 units higher than non-irrigated wheat during the peak of the crop's growing season in the spring (April 7–May 23). In comparison, irrigated corn had NDVI values from 0.12 to 0.16 units higher than non-irrigated corn during the crop's peak greenness and senescence phases in the summer (June 26–September 14). Similar summer NDVI differences were found for sorghum (0.10 to 0.11 NDVI units) and soybeans (0.09 to 0.11 NDVI units) when comparing irrigated and non-irrigated sites. Alfalfa exhibited similar NDVI values between irrigated and non-irrigated sites during the spring (April and May), but considerably higher NDVI values (0.09 to 0.11 NDVI units) on irrigated sites throughout the summer. This larger NDVI difference during the summer reflects the increased level of drought stress that non-irrigated crops commonly experience due to high evapotranspiration rates associated with increased temperature, in conjunction with depleted soil moisture and the higher water demands of a maturing crop. These different spectral–temporal responses exhibited by the irrigated and non-irrigated crops suggest that the time-series MODIS 250 m VI data could potentially be used to discriminate and classify these two land use classes and monitor general crop conditions.

5.2.7. Crop rotations

Multi-temporal NDVI responses of specific crop rotations were also detected in the 12-month time-series of MODIS 250 m data. NDVI profiles for three common winter wheat-related crop rotations are presented in Figure 7. Each rotation had a distinctive NDVI response following winter wheat harvest in late June. The winter wheat-fallow rotation maintained a low post-harvest NDVI value ($\sim$ 0.30) due to the non-vegetated spectral signal from these idle fields. The continuous winter wheat rotation also maintained low post-harvest NDVI values, but exhibited a second minor NDVI peak in November and December associated with the emergence of a new winter wheat crop. The double cropping sequence had a second major NDVI peak in the late summer that represented the growth of a summer crop (typically soybeans), which was planted immediately after wheat harvest. These results show that several common winter wheat crop rotation sequences can be discriminated in a single year of MODIS 250 m VI data, and the identification of additional rotations (e.g., continuous summer crop, summer crop–winter wheat, and summer crop–fallow) should be possible with multiple years of data.

5.2.8. Regional intra-crop VI profiles

Regional variations were found in the multi-temporal VI signatures of individual crops in the MODIS 250 m data that reflected the range of climatic conditions and management practices that a crop is grown under across Kansas. Specific summer crops exhibited clear regional differences in the timing of their greenup onset that were consistent with the planting time differences of each crop among the four corner USDA ASDs evaluated. In general, the timing of greenup onset for a summer crop lagged by two to three 16-day composite periods across Kansas' southeast-to-northwest (earliest date to latest date) gradient. Figure 8a presents these greenup differences for corn. ASD 90 (southeast) had the earliest greenup (May 9), which reflected the district's early planting date range (March 25–April 25). In contrast, ASD 10 (northwest) had the latest greenup (June 26), which reflected the district's later planting date range (March 25–April 25). The timing of greenup for corn became progressively later in a southeast-to-northwest orientation, which was in general agreement with the different recommended planting date ranges for corn among the four ASDs (Table 2). Similar temporal offsets in the timing of greenup were also found for sorghum and soybeans across the ASDs that had similar agreement with the crops' regional planting time differences.

Alfalfa and winter wheat did not exhibit pronounced regional differences in the timing of their spring greenup. This is shown for winter wheat in Figure 8b, where the four ASD-level VI profiles all displayed a rapid greenup between the March 22 and April 7 composite periods. Alfalfa also had a

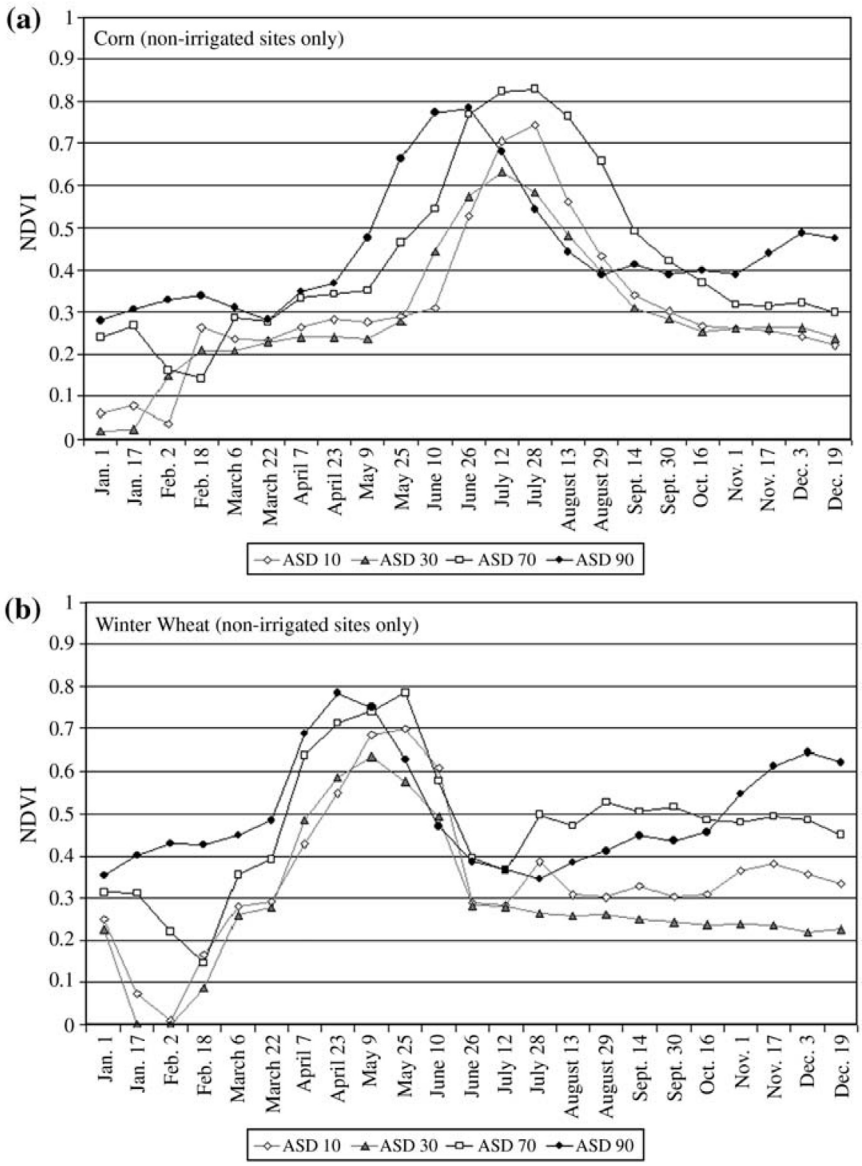

Figure 8. Regional ASD-level NDVI profiles for non-irrigated corn (a) and non-irrigated winter wheat (b). Corn exhibited different timings of greenup among the ASDs that corresponded to the crop's different planting times across Kansas. For winter wheat, all four ASDs experienced greenup onset during the same composite period (between March 22 and April 7). For both crops, higher peak VI values were attained in the eastern ASDs (70 and 90) than the western ASDs (10 and 30) due to higher annual precipitation.

similar rapid greenup in the four ASDs between these same composite periods. The warming of air and soil temperatures in the spring is the primary mechanism that breaks the winter dormancy and triggers plant growth in both crops (Paulsen et al., 1997; Shroyer et al., 1998). These results indicate that the temperature thresholds required to re-initiate plant growth in both crops occurred relatively homogeneously (i.e., within the same 16-day composite period window) across Kansas in 2001.

The influence of Kansas' precipitation gradient was also detected in the MODIS VI data. For each crop, higher peak VI values were consistently detected in the eastern ASDs com-

Table 2. ASD-level planting date ranges recommended for corn

	Observed greenup (MODIS composite period)	Recommended planting date range
ASD 10 (northwest)	June 26	April 20–May 20
ASD 30 (southwest)	June 10	April 15–May 20
ASD 70 (northeast)	May 25	April 1–May 10
ASD 90 (southeast)	May 9	March 25–April 25

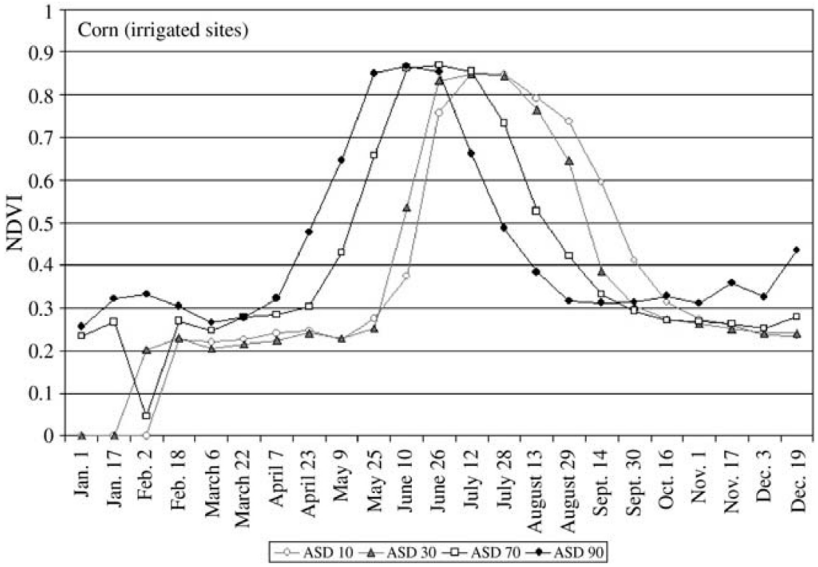

Figure 9. Regional ASD-level NDVI profiles for irrigated corn. Corn had similar peak NDVI values among the ASDs on the irrigated sites, but still exhibited the temporal differences in greenup onset associated with the ASDs' different planting times.

pared to the western ASDs due to increased annual precipitation on the non-irrigated sites. This is illustrated for both corn (Figure 8a) and winter wheat (Figure 8b), where the crops in the eastern ASDs (70 and 90) maintained higher VI values than the western ASDs (10 and 30) throughout most of the growing season. When crops under irrigation were considered, the regional differences in VI values for such crops were considerably reduced among the ASDs. This is illustrated in Figure 9 for irrigated corn, where the peak VI values in the western ASDs (10 and 30) are greatly increased from those of non-irrigated corn (Figure 8a) and are comparable to irrigated corn in the eastern ASDs (70 and 90). However, the temporal offset highlighted earlier for summer crops was still seen in the irrigated sites as demonstrated in Figure 9.

These types of regional, intra-class VI variations detected in the time-series MODIS 250 m data across Kansas represent environmental and management-related sub-classes for each crop type. Such agro-environmental variability should be considered when designing an effective training/validation data sampling scheme or defining smaller, more homogeneous mapping zones for large-area crop classification.

5.3. Inter-class comparison of crop VI profiles

The NDVI profiles in Figure 4 and Figure 5 suggest that the major crop types were separable at different times of the growing season based on their phenologically driven spectral differences. However, these profiles only represent state-level class averages, and as shown earlier, a crop can have considerable intra-class variability across a large geographic area due to variations in environmental conditions and management practices. High intra-class variability can increase the overlap in the VI signals among the crops and reduce their separability. In this section, JM distance calculations, which account for both first order (mean) and second order (variance) distributional properties, were evaluated for crop type pairs to establish their overall separability across the growing season and identify specific periods with the highest separability.

Full-season JM distances (Table 3) showed that alfalfa, winter wheat, and fallow were all highly distinguishable from the other crops when the multi-temporal VI data spanning the growing season are considered. All three crops had JM distances > 1.99 when compared with each of the other crops, which reflects their distinct phenological behaviors. The separability of specific summer crops was lower due to their similar crop calendars. Among the summer crops, corn and soybeans were the most separable (JM = 1.601) and soybeans and sorghum the least separable (JM = 1.278).

When only crops on irrigated sites were considered, the separability between all crop types increased as reflected by the larger JM distances for all crop type pairs. The separability between different non-irrigated crops is reduced by cli-

Table 3. Full growing season JM distance values for all pair-wise crop comparisons, calculated using NDVI time series from non-irrigated and irrigated (in parentheses) field sites

Crop type	Winter wheat	Corn	Soybeans	Sorghum	Fallow
Alfalfa	1.980 (1.999)	1.999 (2)	1.997 (2)	1.994 (2)	2 (2)
Winter wheat	–	1.999 (2)	1.999 (2)	1.998 (2)	1.999 (2)
Corn	–	–	1.601 (1.652)	1.372 (1.952)	1.999 (2)
Soybeans	–	–	–	1.278 (1.933)	2 (2)
Sorghum	–	–	–	–	1.999 (2)

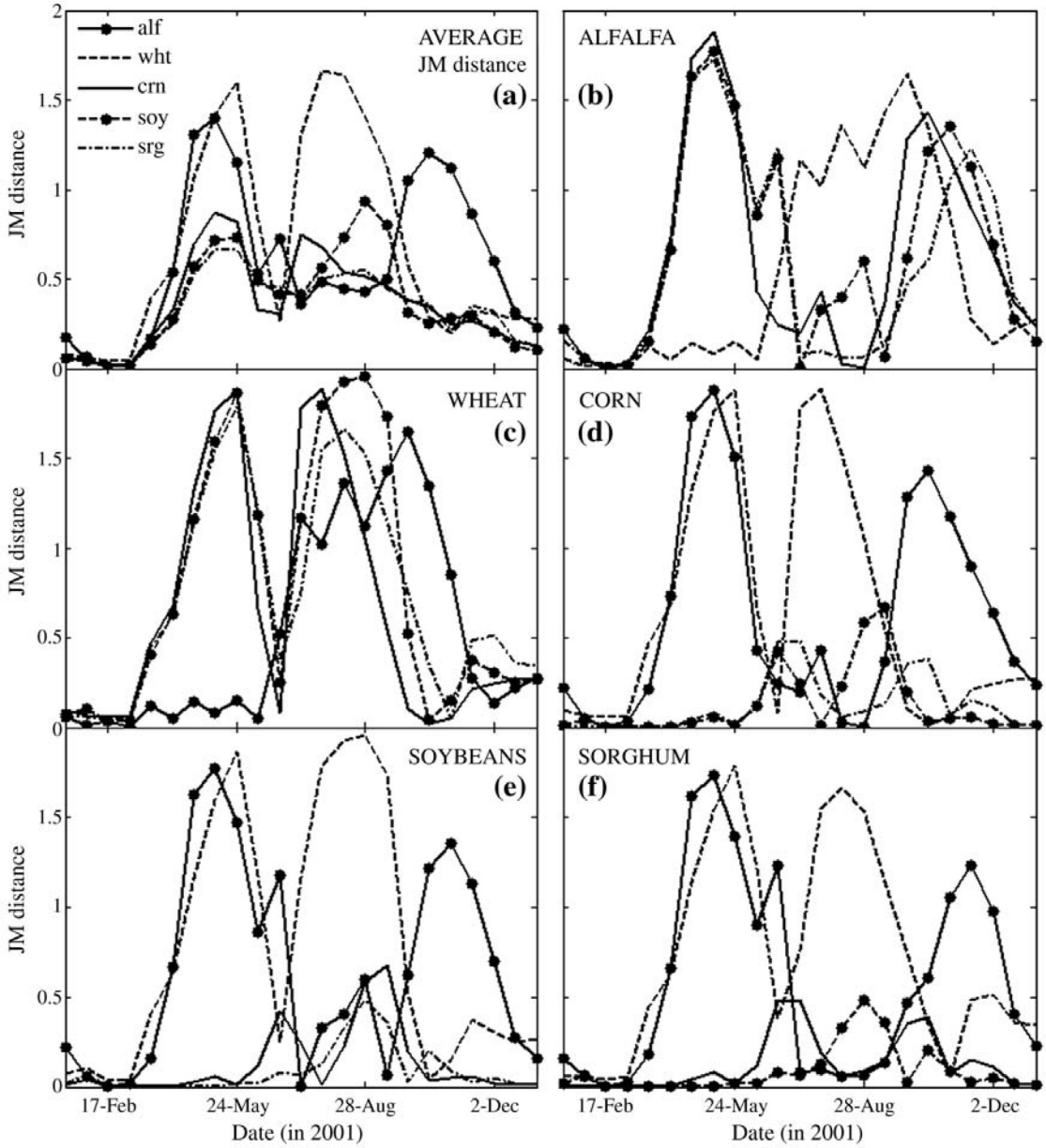

Figure 10. JM distance values observed through pair-wise crop comparisons of field site NDVI, by MODIS time period. Subplot (a) portrays the mean JM distance observed when comparing field site NDVI for each crop to the other four crops, by MODIS time period. As expected, due to their unique crop calendars, alfalfa and wheat demonstrate the greatest overall separability. The crop-specific plots (b)–(f) (the averages of which are depicted in (a)) portray results from the individual pair-wise comparisons. Apparent from these plots is the expected result that the summer crops (corn, soybeans, and sorghum) are not highly separable at any individual time period.

mate-driven, increased variability (and subsequent increased overlap) in their respective VI responses. Sorghum provides the best example of this phenomenon, with a considerable increase in separability from both corn and soybeans when irrigated (JM = 1.952 and 1.933, respectively) than when non-irrigated (JM = 1.372 and 1.278).

Period-by-period mean JM distances (Figure 10a) revealed that alfalfa and winter wheat both had high separability from the other crop types throughout much of the year. Alfalfa (Figure 10b) was highly separable (maximum JM distances > 1.7) from corn, sorghum, and soybeans during the early spring (March to mid-May) when the three summer crops had yet to be planted. Alfalfa and summer crops also had an increased level of separability during the fall (September through November) following the senescence and harvest of the summer crops. Winter wheat and alfalfa were most separable during the summer and fall months following the late June/early July harvest of wheat. Winter wheat (Figure 10c) was clearly discernible from the three summer crops during both the spring (April and May) and summer (July and August) composite periods, with several JM distances from these time spans greater than 1.80. However, the ability to discriminate winter wheat from the summer crops was greatly reduced during the June composite periods (JM dis-

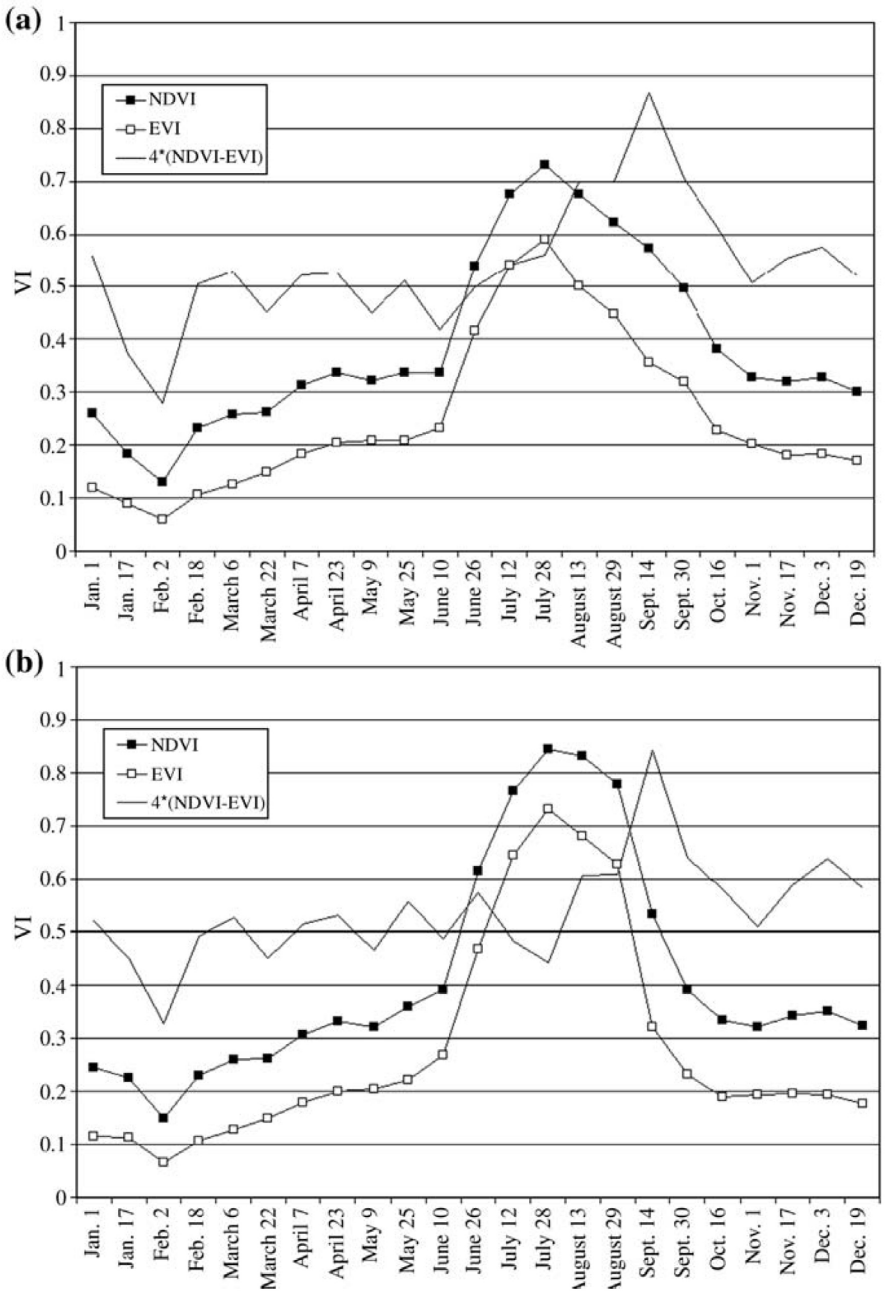

Figure 11. Multi-temporal EVI and NDVI profiles for sorghum (a) and soybeans (b) tracked similar seasonal trajectories, but with greater differences in their response during the senescence phase than during greenup and peak of the crops' growth cycle (apparent from the stretched NDVI–EVI difference series).

tance < 0.5), when winter wheat was in senescence and the summer crops were greening up. The greatest separability among the summer crops occurred during the initial spring greenup phase and/or the late senescence phase. Corn (Figure 10d) had the greatest separability from sorghum and soybeans in both the late June/early July and September composite periods, which reflects the VI differences due to the earlier planting/emergence and senescence of corn. Soybeans (Figure 10e) and sorghum (Figure 10f) were the most separable during August and September, which corresponds to the VI differences between these crops due to their phenology asynchrony and different rates of senescence.

5.4. EVI–NDVI comparisons

5.4.1. Analysis of the multi-temporal EVI–NDVI relationship

A visual comparison of the multi-temporal NDVI and EVI profiles (Figure 4a and b) showed that both VIs depicted similar seasonal events that represented the general phenological characteristics of each crop. For some crops, subtle differences were observed between the EVI and NDVI profiles that were typically restricted to a limited number of composite periods during the peak and/or senescence phases of the growing season. The NDVI was found to maintain higher values than the EVI throughout the year for all crops.

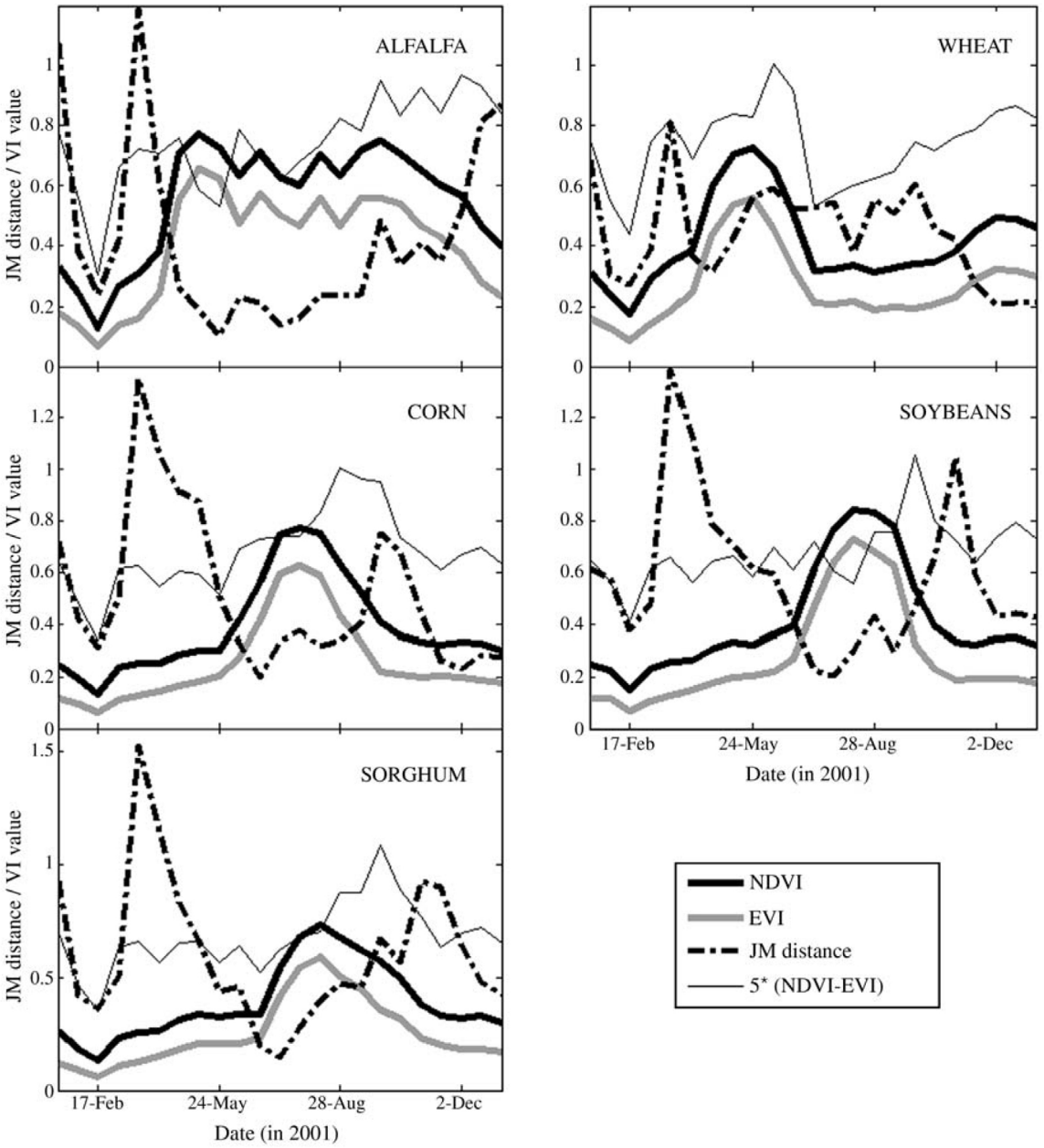

Figure 12. For each crop, the JM distance series comparing field site NDVI and EVI is shown, along with the mean VI series and a stretched difference between the mean VI series. Note that EVI and NDVI demonstrate greater distributional differences during the senescence phase than during greenup.

These results were consistent with the findings of Huete et al. (2002), who found both VIs to have a similar multi-temporal response over a range of biome types, with the NDVI having higher values.

The subtle EVI–NDVI profile differences found for some crops are illustrated for sorghum and soybeans in Figure 11a and b. During the greenup phase, the EVI and NDVI profiles for both crops exhibited similar behavior by increasing at a similar rate. Differences in EVI and NDVI magnitudes were amplified during the senescence phase.

The apparent seasonal EVI–NDVI differences were further explored by investigating the period-by-period correlation, JM distance, and difference between the EVI and NDVI means for each crop. All five crops demonstrated a JM distance time series (Figure 12) that resembled a slightly advanced, inverted VI time series during each crop's active growing season. This indicated that there was more distributional similarity between EVI and NDVI during the crop's growing season than outside the growing season. We note that winter wheat was exceptional in that relatively high JM distance values began reappearing during the peak of the growing season and were sustained throughout the off-season.

With the sole exception of EVI for alfalfa, the JM distance profile intersects the VI profiles at higher VI values during senescence than during greenup for each crop. This re-

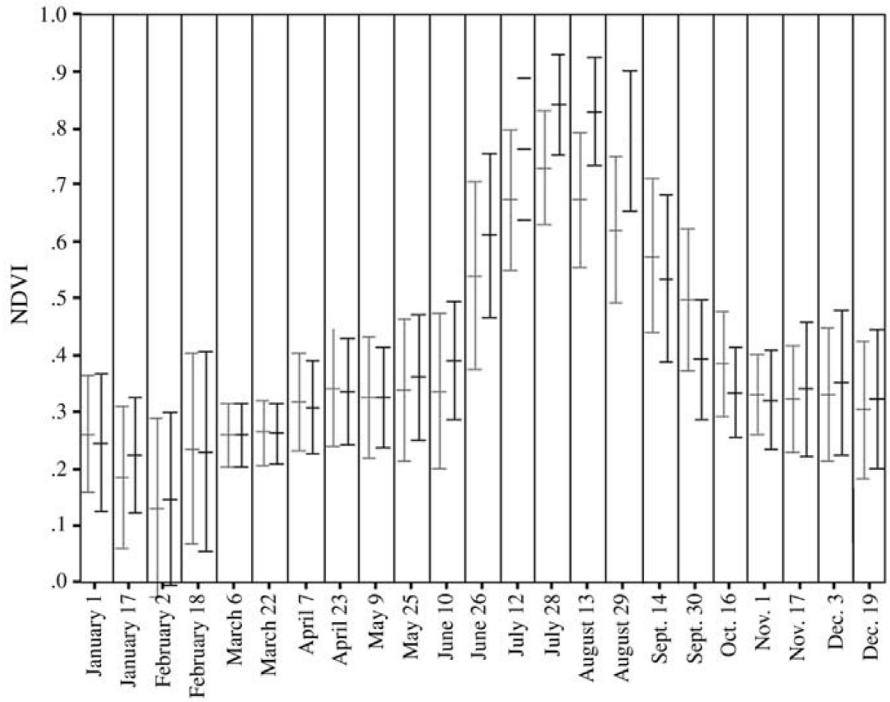

Figure 13. State-level average NDVI values (± 1 S.D.) for sorghum (gray) and soybeans (black). Both crops have a smaller range of values at the very end of their growing season (approximately mid to late October) compared to other composite periods throughout their growth cycle.

sult exposes a tendency for NDVI and EVI to behave more distinctly during senescence than during greenup. The offset between the two VI time series, as represented by the stretched EVI–NDVI difference (5 × (NDVI − EVI)) in Figure 12, also shows the greatest difference in VI values occurred during the senescence phase for all five crops. This partly explains the observed increase in JM distances during this time. However, with the exception of winter wheat, the late-season peak of each JM distance series lags behind the peak of the stretched VI difference profile. Since the offset between the EVI and NDVI series is in decline at the time of the late-season JM distance peak, and considering the JM distance formula, the only possible explanation for this behavior is that the VI profiles demonstrated a reduction in variance at the time of the late peak in the JM distance profiles (i.e., at the end of the growing season). Time series of period-specific standard deviations of crop-specific EVI and NDVI values confirm this hypothesis, as shown for sorghum and soybeans in Figure 13.

All crops had high EVI–NDVI correlations (> 0.90) in both the greenup and senescence phases (Table 4), with the exception of winter wheat, which had slightly lower correlations (0.85 and 0.69). The lower correlation values for winter wheat could be due to variations in the VIs associated with the post-harvest spectral background response from the harvested wheat fields in the July 12 composite period, which was included so both phases would have an equal number of periods for correlation. Each crop had a lower correlation for the senescence phase than the greenup phase. This result was consistent with the previously noted mean differences and the JM distance results, which both indicated more distinct behavior during senescence than during greenup. Another observed result was that the correlations were lower in both phases for all crops on the non-irrigated sites than the irrigated sites, reflecting the expected differences in crop growth variability under these two management practices.

This series of EVI–NDVI analyses indicates that the two VIs had greater differences in their responses to vegetation condition changes during senescence compared to the other phases of the growing season for the five crops. For example, the EVI decreased more rapidly than the NDVI at the onset of senescence for most crops. Had this difference been primarily due to the increased sensitivity of EVI compared to NDVI for higher VI values, then a similar pattern would have been observed during the transition from the greenup phase to peak season (it was not). Rather, the EVI–NDVI differences during this "dry down" period are probably biologically driven, and may be partially attributed to the sensitiv-

Table 4. Greenup and senescence phase EVI–NDVI correlations (I = irrigated, NI = non-irrigated)

	Alfalfa (I)	Alfalfa (NI)	Corn (I)	Corn (NI)	Sorghum (I)	Sorghum (NI)	Soybeans (I)	Soybeans (NI)	Winter wheat (I)	Winter wheat (NI)
Greenup phase	0.964	0.947	0.982	0.978	0.983	0.970	0.964	0.947	0.982	0.978
Senescence phase	0.955	0.903	0.967	0.965	0.907	0.907	0.955	0.903	0.967	0.965

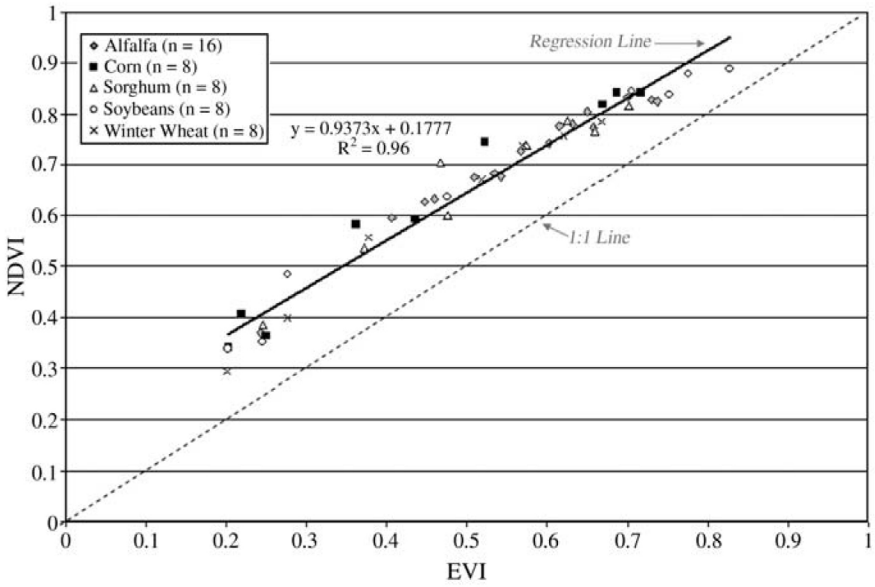

Figure 14. Crossplot of the multi-temporal EVI and NDVI data, with each point representing the average, crop-specific VI values from a single MODIS composite during each crop's growth cycle (n = length of growing season, in MODIS periods). Though the multi-temporal VI responses were highly correlated ($R^2 = 0.96$), the NDVI had reduced sensitivity and began to approach an asymptotic level at high biomass levels (e.g., NDVI > 0.80) relative to the EVI. Likewise, EVI demonstrated reduced sensitivity at low biomass levels (e.g., NDVI < 0.50) relative to NDVI.

ity of the VI's to different physiological changes (i.e., changes in leaf structure versus chlorophyll concentration) (Gao et al., 2000) in the crops. The EVI–NDVI variations did not appear to be the result of the canopy background signal being removed in the EVI calculations. Both VIs exhibited a similar behavior and had higher correlations during the greenup phase (i.e., crop emergence) when the non-photosynthetically active soil/crop residue background would have its greatest contribution to the growing season spectral signal. Additional research is needed to investigate the subtle seasonal difference in the EVI–NDVI relationship that was observed in this study between the greenup and senescence phases for all crops.

5.4.2. EVI–NDVI crossplot

A crossplot of the multi-temporal EVI and NDVI data (based on period-by-period, crop-specific state-level averages) showed that the two VIs had a slight curvilinear relationship across the growing season (Figure 14). At the highest VI values, which correspond to the peak growing season conditions of the crops, the NDVI exhibited less signal variation than the EVI and appeared to approach an asymptotic level near 0.90. The NDVI exhibited a range of values between 0.80 and 0.88 at the time of peak green biomass for all crops. In comparison, the EVI captured more variability in the vegetation changes of the crops at that time by maintaining a larger range of values (0.60 to 0.82). This result was consistent with the EVI's design, which was intended to have improved sensitivity to vegetation changes over high biomass areas as compared to the NDVI, which tends to saturate (Huete et al., 1994). Huete et al. (2002) also found similar EVI–NDVI relationship at the higher values over several biome types. On the other hand, the increased sensitivity of NDVI compared to EVI at lower VI levels is also apparent, both in Figure 14 and in the dynamic ranges of the late-season, new-crop winter wheat responses found at the end of the "winter wheat" and "fallow" profiles shown in Figure 4a and b. Considering the equations for NDVI and EVI (see (1) and (2)), it seems likely that the inclusion of the blue band in the EVI calculations is partly responsible for the EVI–NDVI differences that were observed. Further research is needed to determine the exact extent of the blue band's influence on the observed EVI–NDVI relationship.

6. Conclusions

The objective of this research was to evaluate the applicability of time-series MODIS 250 m VI data for large-area crop-related LULC classification in the U.S. Central Great Plains region. From this work, we drew several conclusions regarding the suitability of the data for this specific application.

First, we concluded that a time-series of the 16-day composite MODIS 250 m VI data had sufficient spectral, temporal, and radiometric resolutions to discriminate the region's major crop types and crop-related land use practices. For each crop, a unique multi-temporal VI profile was detected in the MODIS 250 m data that was consistent with the known crop phenology. Most crop classes were separable at some point during the growing season based on their phenology-driven spectral–temporal differences expressed in the VI data.

Second, we found that regional intra-class variations were detected in the VI data that reflected the climate and planting date gradient across Kansas. The VI profiles for each summer crop type were temporally offset by one or more 16-day composite periods, which reflected the crops' different regional planting times. Regional differences in the

peak VI values, which followed the state's pronounced precipitation gradient, were found among the four corner ASDs for each crop type when the non-irrigated sites were evaluated. However, these peak VI differences were substantially reduced for the crops on irrigated field sites. These regional intra-class variations represent sub-classes for each crop at the state level and must be addressed in the development of a large-area crop mapping methodology. These types of regional variations need to be considered during the selection of training samples prior to classification to ensure that both the climate and management-related sub-classes within each crop class are represented in the training set. The delineation of relatively homogeneous crop mapping zones or "agro-regions" (i.e., areas with similar cropping practices and environmental conditions), as well as the use of non-parametric classifiers (e.g., decision tree) that can handle an information class with multiple sub-classes, are two analytical approaches capable of accommodating this intra-class variability. The sensitivity of the MODIS VI to these regional variations also illustrates the considerable potential of these data for crop condition monitoring and phenology studies (Wardlow et al., 2006).

Third, we determined that MODIS' 250 m spatial resolution was an appropriate scale at which to map the general cropping patterns of the U.S. Central Great Plains. Similar cropping patterns were visually resolved in both the MODIS 250 m and Landsat ETM+ 30 m imagery throughout Kansas. The spatial pattern of fields 32.4 ha or larger was generally resolvable at the 250 m resolution. "Mixed" pixels of multiple land cover or crop types may be an issue for some locations or classes. However, the sub-pixel unmixing of the proportions of specific land cover and/or crop types from the MODIS 250 m VI data may be possible (Lobell & Asner, 2004).

Lastly, we found that the MODIS EVI and NDVI both depicted similar seasonal variations and were highly correlated for all crops. However, we did find a few subtle but consistent differences between the two VIs. The VIs behaved more distinctly in their response during senescence than during greenup and peak season. With little exception, this phenomenon was found for all crops using multiple analysis methods. The VIs also exhibited a curvilinear relationship near the extremes of the VI value ranges. For example, the NDVI began to approach an asymptotic level at the peak of the growing season (i.e., at maximum VI values), whereas the EVI exhibited more sensitivity during this growth stage. In summary, the greater sensitivity of NDVI across the low to intermediate green biomass levels may capture more subtle variations among crops during early greenup and late senescence phases, whereas the EVI may be more appropriate for separating crops at the peak of the growing season.

Time-series MODIS 250 m VI data offer new opportunities for detailed, large-area crop mapping given their unique combination of resolutions, geographic coverage, and cost. This research has shown the wealth of crop-related LULC information in the MODIS 250 m VI products and has illustrated the potential of these data for detailed crop characterization. The next step is to test the capability of the time-series MODIS 250 m EVI and NDVI data for mapping detailed, regional-scale, crop-related LULC patterns in the U.S. Central Great Plains. The MODIS VI data should also be tested for mapping specific crop rotation sequences and other rapid agricultural land cover changes such as the USDA Conservation Reserve Program (CRP) cropland/grassland conversions. Beyond classification, the use of the MODIS VI data should be expanded to monitor regional crop conditions, a task that will become increasingly tenable as more years of data are collected and the historical MODIS VI record needed for baseline establishment grows. The integration of the crop-related LULC classifications and vegetation condition information that can be extracted from the MODIS 250 m VI data would form a potentially powerful monitoring tool to assess regional variations in the general conditions of specific crop types and identify localized areas of vegetation stress in a similar fashion to the variety of AVHRR NDVI-based environmental monitoring efforts summarized by McVicar and Jupp (1998). The results from this study are intended to provide a basis upon which future research can build to develop large-area LULC datasets and tools that characterize the cropland sector.

Acknowledgments

This research was supported by NASA Headquarters under the Earth System Science Fellowship Grant NGT5-50421 and the USGS AmericaView program. The work was conducted at the Kansas Applied Remote Sensing (KARS) Program (Edward A. Martinko, Director; Kevin P. Price, Associate Director). The authors thank the Kansas Farm Service Agency and 48 of its county offices for providing the annotated aerial photographs used for field site selection. The authors also thank the three anonymous reviewers for their constructive comments and suggestions regarding this manuscript.

References

Asrar et al., 1989 • G. Asrar, R. B. Myneni, and E. T. Kanemasu, Estimation of plant canopy attributes from spectral reflectance measurements: Chapter 7. In: G. Asrar, Editor, *Theory and applications of optical remote sensing*, Wiley Publishers, New York (1989), pp. 252–296.

Baret and Guyot, 1991 • F. Baret and G. Guyot, Potentials and limits to vegetation indices for LAI and APAR assessments, *Remote Sensing of Environment* **35** (1991), pp. 161–173.

Cihlar, 2000 • J. Cihlar, Land cover mapping of large areas from satellites: Status and research priorities, *International Journal of Remote Sensing* **21** (2000) (6–7), pp. 1093–1114.

Craig, 2001 • M. E. Craig, The NASS cropland data layer program Third Annual International Conference on Geospatial Information in Agriculture, Denver, CO, November 5–7 (2001).

DeFries and Belward, 2000 • R. S. DeFries and A. S. Belward, Global and regional land cover characterization from satellite data: An introduction to the special issue, *International Journal of Remote Sensing* **21** (2000) (6–7), pp. 1083–1092.

DeFries et al., 1998 • R. S. DeFries, M. C. Hansen, J. R. G. Townshend, and R. S. Sohlberg, Global land cover classifications at 8 km spatial resolution: The use of training data derived from Landsat imagery in decision tree classifiers, *International Journal of Remote Sensing* **19** (1998), pp. 3141–3168.

DeFries and Townshend, 1994 • R. S. DeFries and J. R. G. Townshend, NDVI-derived land cover classifications at a global scale, *International Journal of Remote Sensing* **15** (1994), pp. 3567–3586.

Eve and Merchant, 1998 • M. D. Eve and J. W. Merchant (1998). *National Survey of Land Cover Mapping Protocols Used in the GAP Analysis Program*. GAP Land Cover Mapping Protocols homepage, Center for Advanced Land Management Information Technologies (CALMIT), University of Nebraska-Lincoln, Lincoln, NE; http://www.calmit.unl.edu/gapmap/ (accessed August 5, 2005).

Gao et al., 2000 • X. Gao, A. R. Huete, W. Ni, and T. Miura, Optical–biophysical relationships of vegetation spectra without background contamination, *Remote Sensing of Environment* **74** (2000), pp. 609–620.

Hansen et al., 2000 • M. C. Hansen, R. S. DeFries, J. R. G. Townshend, and R. Sohlberg, Global land cover classification at 1 km spatial resolution using a classification tree approach, *International Journal of Remote Sensing* **21** (2000) (6–7), pp. 1331–1364.

Hansen et al., 2002 • M. C. Hansen, R. S. DeFries, J. R. G. Townshend, R. Sohlberg, C. Dimiceli, and M. Carroll, Towards an operational MODIS continuous field of percent tree cover algorithm: Examples using AVHRR and MODIS data, *Remote Sensing of Environment* **83** (2002), pp. 303–319.

Havlin et al., 1995 • J. Havlin, A. Schlegel, K. C. Dhuyvetter, J. P. Shroyer, H. Kok, and D. Peterson, *Great plains dryland conservation technologies*, *Publication* Vol. S-81, Kansas State University, Manhattan, KS (1995, June), pp. 7–11.

Homer et al., 2004 • C. Homer, C. Huang, L. Yang, B. Wylie, and M. Coan, Development of a 2001 national land-cover database for the United States, *Photogrammetric Engineering and Remote Sensing* **70** (2004) (7), pp. 829–840.

Huete et al., 2002 • A. Huete, K. Didan, T. Miura, E. P. Rodriguez, X. Gao, and L. G. Ferreira, Overview of the radiometric and biophysical performance of the MODIS vegetation indices, *Remote Sensing of Environment* **83** (2002), pp. 195–213.

Huete et al., 1994 • A. Huete, C. Justice, and H. Liu, Development of vegetation and soil indices for MODIS–EOS, *Remote Sensing of Environment* **49** (1994), pp. 224–234.

Huete et al., 1999 • A. Huete, C. Justice, and W. van Leeuwen, *MODIS vegetation index (MOD 13) algorithm theoretical basis document (ATBD) Version 3. 0. EOS Project Office*, NASA Goddard Space Flight Center, Greenbelt, MD (1999), p. 2.

Huete et al., 1997 • A. Huete, H. Q. Liu, K. Batchily, and W. van Leeuwen, A comparison of vegetation indices over a global set of TM images for EOS–MODIS, *Remote Sensing of Environment* **59** (1997), pp. 440–451.

IGBP, 1990 • IGBP, The International Geosphere–Biosphere Programme: A study of global change – The initial core projects, *IGBP global change report no. 12, International Geosphere–Biosphere Programme, Stockholm, Sweden* (1990).

Jakubauskas et al., 2002 • M. E. Jakubauskas, D. L. Peterson, J. H. Kastens, and D. R. Legates, Time series remote sensing of landscape–vegetation interactions in the southern Great Plains, *Photogrammetric Engineering and Remote Sensing* **68** (2002) (10), pp. 1021–1030.

Justice and Townshend, 2002 • C. O. Justice and J. R. G. Townshend, Special issue on the Moderate Resolution Imaging Spectroradiometer (MODIS): A new generation of land surface monitoring, *Remote Sensing of Environment* **83** (2002), pp. 1–2.

Lobell and Asner, 2004 • D. B. Lobell and G. P. Asner, Cropland distributions from temporal unmixing of MODIS data, *Remote Sensing of Environment* **93** (2004), pp. 412–422.

Loveland and Belward, 1997 • T. R. Loveland and A. S. Belward, The IGBP–DIS global 1 km land cover data set, DISCover: First results, *International Journal of Remote Sensing* **18** (1997) (15), pp. 3289–3295.

Loveland et al., 1991 • T. R. Loveland, J. W. Merchant, D. O. Ohlen, and J. F. Brown, Development of a land cover characteristics database for the conterminous U. S, *Photogrammetric Engineering and Remote Sensing* **57** (1991) (11), pp. 1453–1463.

Loveland et al., 1995 T. R. Loveland, J. W. Merchant, B. C. Reed, J. F. Brown, D. O. Ohlen, and P. Olson *et al.,* Seasonal land cover regions of the United States, *Annals of the Association of American Geographers* **85** (1995), pp. 339–355.

Loveland et al., 2000 • T. R. Loveland, B. C. Reed, J. F. Brown, D. O. Ohlen, Z. Zhu, and L. Yang *et al.,* Development of a global land cover characteristics database and IGBP DISCover from 1 km AVHRR data, *International Journal of Remote Sensing* **21** (2000) (6–7), pp. 1303–1330.

Lu et al., 2003 • H. Lu, M. R. Raupach, T. R. McVicar, and D. J. Barrett, Decomposition of vegetation cover into woody and herbaceous components using AVHRR NDVI time series, *Remote Sensing of Environment* **86** (2003) (1), pp. 1–18.

McVicar and Jupp, 1998 • T. R. McVicar and D. L. B. Jupp, The current and potential operational uses of remote sensing to aid decisions on drought exceptional circumstances in Australia: A review, *Agricultural Systems* **57** (1998), pp. 399–468.

Morton et al., 2006 • D. C. Morton, R. S. DeFries, Y. E. Shimabukuro, L. O. Anderson, E. Arai, and F. B. Espirito-Santo *et al.,* Cropland expansion changes deforestation dynamics in the southern Brazilian Amazon, *Proceedings of the National Academy of Sciences of the United States of America* **103** (2006) (39), pp. 14637–14641.

Mosiman, 2003 • Mosiman, B. (2003). Exploring Multi-Temporal and Transformation Methods for Improved Cropland Classification Using Landsat Thematic Mapper Imagery. Master's Thesis, Department of Geography, University of Kansas, Lawrence, KS.

National Aeronautics and Space Administration (NASA), 2002 • National Aeronautics and Space Administration (NASA) (2002). *NASA's Land Cover Land Use Change (LULCC) Program*, NASA LCLUC webpage, University of Maryland, College Park, MD; http://lcluc.umd.edu (accessed December 12, 2005).

National Research Council (NRC), 2001 • National Research Council (NRC), *Grand challenges in environmental sciences,* National Academy Press, Washington, DC (2001).

Paulsen et al., 1997 • G. M. Paulsen, J. P. Shroyer, J. Kok and C. R. Thompson, *Wheat production guide., Publication* Vol. C-529, Kansas State University, Manhattan, KS (1997, May), pp. 2–11.

Price et al., 1997 • K. P. Price, S. L. Egbert, M. D. Nellis, R. Y. Lee, and R. Boyce, Mapping land cover in a high plains agro-ecosystem using a multidate landsat thematic mapper modeling approach, *Transactions of the Kansas Academy of Science* **100** (1997) (1–2), pp. 21–33.

Reed et al., 1994 • B. C. Reed, J. F. Brown, D. VanderZee, T. R. Loveland, J. W. Merchant, and D. O. Ohlen, Measuring phenological variability from satellite imagery, *Journal of Vegetation Science* **5** (1994), pp. 703–714.

Reed et al., 1996 • B. C. Reed, T. R. Loveland, and L. L. Tieszen, An approach for using AVHRR data to monitor U. S. Great Plains grasslands, *Geocarto International* **11** (1996) (3), pp. 13–22.

Richards and Jia, 1999 • J. A. Richards and X. Jia, Remote sensing digital image analysis (3rd ed.), Springer-Verlag, Berlin (1999).

Rogers, 1997 • D. H. Rogers, *Soybean production handbook., Publication* Vol. C-449, Kansas State University, Manhattan, KS (1997, March), pp. 15–19.

Sarmiento and Wofsy, 1999 Sarmiento, J. L. & Wofsy, S. C. (co-editors), (1999). *A U. S. Carbon Cycle Science Plan*. U. S. Global Change Research Program, Washington, DC, pp. 29–31.

Shroyer et al., 1998 • J. P. Shroyer, P. C. St. Amand, and C. Thompson, *Alfalfa production handbook., Publication* Vol. C-683, Kansas State University, Manhanttan, KS (1998, October), pp. 3–12.

Shroyer et al., 1996 • J. P. Shroyer, C. Thompson, R. Brown, P. D. Ohlenbach, D. L. Fjell, and S. Staggenborg *et al., Kansas crop planting guide., Publication* Vol. L-818, Kansas State University, Manhattan, KS (1996, November), p. 2.

Townshend and Justice, 1988 • J. R. G. Townshend and C. O. Justice, Selecting the spatial resolution of satellite sensors required for global monitoring of land transformations, *International Journal of Remote Sensing* **9** (1988) (2), pp. 187–236.

Turner et al., 1995 • B. L. Turner II, D. Skole, S. Sanderson, G. Fischer, L. Fresco, and R. Leemans (1995). *Land-Use and Land-Cover Change Science/Research Plan*. IGBP Report No. 35 and HDP Report No. 7.

USDA, 2002 • USDA (2002). *Kansas Farm Facts 2002*. USDA NASS Kansas Agricultural Statistical Office homepage, Topeka, KS; http://www.nass.usda.gov.ks/ (accessed June 13, 2005).

USDA, 2004 • USDA (2004). *Frequently Asked Questions (FAQs) Related to the USDA–NASS Quick Stats County Data*. USDA NASS Quick Stats Agricultural Statistics Database webpage, http://www.nass.usda.gov:81/ipedbcnty/faqs.htm-frequency (accessed August 23, 2005).

Vanderlip and Fjell, 1994 • R. L. Vanderlip and D. L. Fjell, *Corn production handbook., Publication* Vol. C-560, Kansas State University, Manhattan, KS (1994, May), pp. 23–27.

Vanderlip et al., 1998 • R. Vanderlip, D. H. Rogers, and M. Alam, *Grain sorghum production guide., Publication* **Vol. C-687**, Kansas State University, Manhattan, KS (1998, May), pp. 15–18.

Van Niel and McVicar, 2004 • T. G. Van Niel and T. R. McVicar, Determining temporal windows of crop discrimination with remote sensing: A case study in south-eastern Australia, *Computers and Electronics in Agriculture* **45** (2004), pp. 91–108.

Van Niel et al., 2005 • T. G. Van Niel, T. R. McVicar, and B. Datt, On the relationship between training sample size and data dimensionality: Monte Carlo analysis of broadband multi-temporal classification, *Remote Sensing of Environment* **98** (2005), pp. 468–480.

Vogelmann et al., 2001 J. E. Vogelmann, S. M. Howard, L. Yang, C. R. Larson, B. K. Wylie, and J. N. Van Driel, Completion of the 1990's National Land Cover data set for the conterminous United States, *Photogrammetric Engineering and Remote Sensing* **67** (2001), pp. 650–662.

Wardlow et al., 2006 • B. D. Wardlow, J. H. Kastens, and S. L. Egbert, Using USDA crop progress data for the evaluation of greenup onset date calculated from MODIS 250-meter data, *Photogrammetric Engineering and Remote Sensing* **72** (2006) (11), pp. 1225–1234.

Wessels et al., 2004 • K. J. Wessels, R. S. DeFries, J. Dempewolf, L. O. Anderson, A. J. Hansen, and S. L. Powell *et al.,* Mapping regional land cover with MODIS data for biological conservation: Examples from the Great Yellowstone Ecosystem, USA and Para State, Brazil, *Remote Sensing of Environment* **92** (2004), pp. 67–83.

Wolfe et al., 2002 • R. E. Wolfe, M. Hishihama, A. J. Fleig, J. A. Kuyper, D. P. Roy, and J. C. Storey *et al.,* Achieving sub-pixel geolocation accuracy in support of MODIS land science, *Remote Sensing of Environment* **83** (2002), pp. 31–49.

Zhan et al., 2000 • X. Zhan, R. DeFries, J. R. G. Townshend, C. Dimiceli, M. Hansen, and C. Huang *et al.,* The 250 m global land cover change product from the Moderate Resolution Imaging Spectroradiometer of NASA's Earth Observing System, *International Journal of Remote Sensing* **21** (2000) (6–7), pp. 1433–1460.

Zhan et al., 2002 • X. Zhan, R. A. Sohlberg, J. R. G. Townshend, C. DiMiceli, M. L. Carroll, and J. C. Eastman *et al.,* Detection of land cover changes using MODIS 250 m data, *Remote Sensing of Environment* **83** (2002), pp. 336–350.

Zhang et al., 2003 • X. Zhang, M. A. Friedl, C. B. Schaaf, A. H. Strahler, J. C. F. Hodges, and F. Gao *et al.,* Monitoring vegetation phenology using MODIS, *Remote Sensing of Environment* **84** (2003), pp. 471–475.